Krill (*Meganyctiphanes norvegica*) diel vertical migration and individual daytime behavior

An acoustic study

Fredrik Lund Moksnes

Master Thesis
Section for Aquatic Biology and Toxicology (AKVA)

Department of Biosciences
Faculty of Mathematics and Natural Sciences

UNIVERSITY OF OSLO

November 2021

Krill (*Meganyctiphanes norvegica*) diel vertical migration and individual daytime behavior: *An acoustic study*

Master thesis written by Fredrik Lund Moksnes at Department of Biosciences, Section for Aquatic Biology and Toxicology (AKVA), Faculty of Mathematics and Natural Sciences (MATNAT), University of Oslo. Submitted November 2021.

2021

Krill (*Meganyctiphanes norvegica*) diel vertical migration and individual daytime behavior: *An acoustic study*

Author: Fredrik Lund Moksnes

http://www.duo.uio.no/

Trykk: Reprosentralen, Universitetet i Oslo

Abstract

Krill are important organisms in the world's oceans. They are present in all of them and make up a large portion of the zooplanktonic biomass. *Meganyctiphanes norvegica* are one of the species that participate in diel vertical migrations (DVM), a large-scale pattern of migrating up to shallow depths during night, and down to greater depths by day. This behavior is associated with food search and predator avoidance respectively. Although there is an abundance of krill in all oceans, little is still known about their activities during the day, because *in situ* studies in proximity of their populations have been difficult to implement. My goal was to study behavioral patterns of a population of *M. norvegica*, as well as individual behaviors during their daytime distribution in the deep waters of a fjord system.

We deployed an autonomous upwards-facing split beam echosounder at the bottom of a sheltered location in the Oslofjord, Norway. Short-term records were collected from three seasons: spring, summer, and autumn. We supplemented the acoustic data with intermittent field sampling and environmental profiles.

The krill population always conducted DVM. The duration of the daytime distribution at depth varied with seasonality, i.e., with day length, but not within the same season. Submerging the echosounder at depth close to the population enabled studying individual krill during the day. Their behaviors varied between recording periods. In late spring, subsequent a phytoplankton bloom, they sank by spiraling in circles down to the seabed. We suggest that this behavior is associated with grazing on deep sinking algae. The krill subsequently swam back up and repeat the behavior several times during the day. These discoveries are of consequence for the biological pump, the krill energy budget, and their association with isolumes. In late summer, krill swam more actively, alternating between going up and diving downwards. We suspect this behavior is associated with a switch in food preference, the krill now to a larger extent foraging as a carnivore. In autumn the summer behavioral pattern persists, but now occurred higher up in the water column due to oxygen constraints in deeper waters. The deepest daytime range of *M. norvegica* suggests a lower tolerance of ~0.67 mg/l.

Fish was only observed in the upper part of the krill layer, deep-going krill seemingly avoiding planktivores. Krill in upper parts of the daytime layer had to escape diving fish. Also, while krill were forced upwards from the deep following reduced oxygen levels, the same seemed to apply for fish.

Acknowledgements

My favorite subject during my undergraduate years was behavioral ecology. Mixed with a fascination of the oceans and marine life, I was lucky enough to get to write a thesis about both. Before starting on this journey, I knew very little about the pelagic realm and the use of echosounders as a tool in marine research. I hope that this process has provided me with valuable knowledge for the future, even though the more I learn, the more I become aware of how little I know.

I would like to take this opportunity to thank my supervisor, Professor Stein Kaartvedt, for teaching me how to write science properly, for his supervision during field campaigns, always ensuring educational content, and to always be available, even in times when we couldn't meet in person. I would like to thank research fellow Svenja Christiansen for always being available for technical support, and for being my software wizard. I would like to thank head engineer Rita Amundsen for her guidance in the lab.

Thanks to all my study buddies in room 4605 that made these years most memorable, with special thanks to Ovin Holm for his support, both academically and socially.

Most of all I would like to thank my parents, and my partner Nora, for their unconditional love and support through these years. I would never have gotten through this without it.

Table of contents

1 Introduction

1.1 Krill

The northern krill (*Meganyctiphanes norvegica*) is a species of euphausiids (Order Euphausiacea), which is a classification of pelagic organisms that are shrimp-like in appearance (Brusca et al., 2016). Krill are in general important players in the food web, are present in all major oceans and make up a significant portion of the global zooplankton biomass (Brusca et al., 2016; Denny, 2008). Commonly found in boreal North Atlantic (Dalpadado & Skjoldal, 1991; Tarling et al., 2010), *M. norvegica* (Fig. 1) is abundant in fjord systems, and in the Oslofjord they can be studied *in situ* through acoustic studies of the water column. The northern krill carries out diel vertical migrations (DVM), ascending to upper waters around sunset, and retreat to the depths at sunrise. However, closer looks into this reveal variations to this simplified pattern (Kaartvedt, 2010).

Fig. 1. *Meganyctiphanes norvegica*, ~3- 4 cm long. [Photo: F. L. Moksnes]

1.2 Diel Vertical Migrations

Diel vertical migration (DVM) is a behavioral pattern of daily, and nightly movement of organisms up and down the water column (Berge et al., 2014; Hays, 2003). DVM patterns are normally ascribed to foraging in upper waters at night and hiding from predators in the deep, darker waters by day. In some locations, it has been observed that *M. norvegica* always carry out DVM (Sourisseau et al., 2008), while part of the population may remain in deep waters at night at other locations (Kaartvedt, 2010). DVM has been referred to as possibly the largest

migration on earth and is of significance on a global scale because it supports in transporting carbon from upper to deeper waters and may as such play a role in hampering climate change, through its impact on the biological pump (Archibald et al., 2019; Ringelberg, 2010). Little however is known about the behaviors of individual krill when they are in their daytime habitats, and this is largely due to methodological constraints (Kaartvedt, 2010). It has been found that krill, including *M. norvegica*, display a lower swimming velocity during the day (De Robertis et al., 2003; Klevjer & Kaartvedt, 2011). Their daytime vertical distribution varies by light conditions (Onsrud & Kaartvedt, 1998), their size may increase with depth (Klevjer & Kaartvedt, 2006), and increasing size seems to have a positive effect on the swimming capacity of *M. norvegica* (Thomasson et al., 2003). Some three dimensional swimming patterns have been established in Klevjer & Kaartvedt (2006). While generally considered to forage in upper waters at night (Kaartvedt, 2010), it has also been found that krill graze on algae in their daytime habitat when available, such as during spring (Onsrud & Kaartvedt, 1998), as well as foraging on copepods as visual predators (Kaartvedt et al., 2002; Torgersen, 2001). When hunting it has been reported asymmetry in the direction to where they attack prey (Abrahamsen et al., 2010). It is also known that *M. norvegica* has a high mortality in anoxic waters and generally avoid waters that has become increasingly hypoxic over time, as can be the case in fjords (Beyer, 1968; Røstad & Kaartvedt, 2013; Solberg et al., 2015; Spicer et al., 1999).

1.3 Fjords

Fjords are inlets of seawater from coastal areas. A fjord is a type of estuary that appear in areas where there previously have been glaciers (Kaartvedt, personal communication). Thus, we usually find fjords in temperate to polar regions. The fjord basin can be quite deep, stretching down to over 1300 meters depth in one case (Holtedahl, 1967; Nesje & Whillans, 1994). The threshold between coastal waters and the inlet (also called a sill) can be quite shallow isolating waters in the fjord from the coastal waters. This causes environments in the fjord basin to be very different from the environment in the open sea, hence also its ecology. A fjord is often brackish, meaning that its upper waters are freshwater influenced from surrounding inputs of freshwaters such as rivers, lakes, and runoff from land. Since the sill has such a shallow depth, water exchange is often limited to the upper layer. Oxygen is consumed over time, and conditions in the deep fjord waters can become hypoxic. This is

particularly the case for the inner Oslofjord (Fig. 2), where a second sill further hampers the water exchange. Another variable that is special about the Oslofjord is high light attenuation causing dark waters at shallow depths (Frigstad et al., 2020). Fjord effects like these make them convenient model systems for deep ocean comparisons, and krill studies can be conducted without much of the logistical issues associated with open ocean research (Kaartvedt, personal communication).

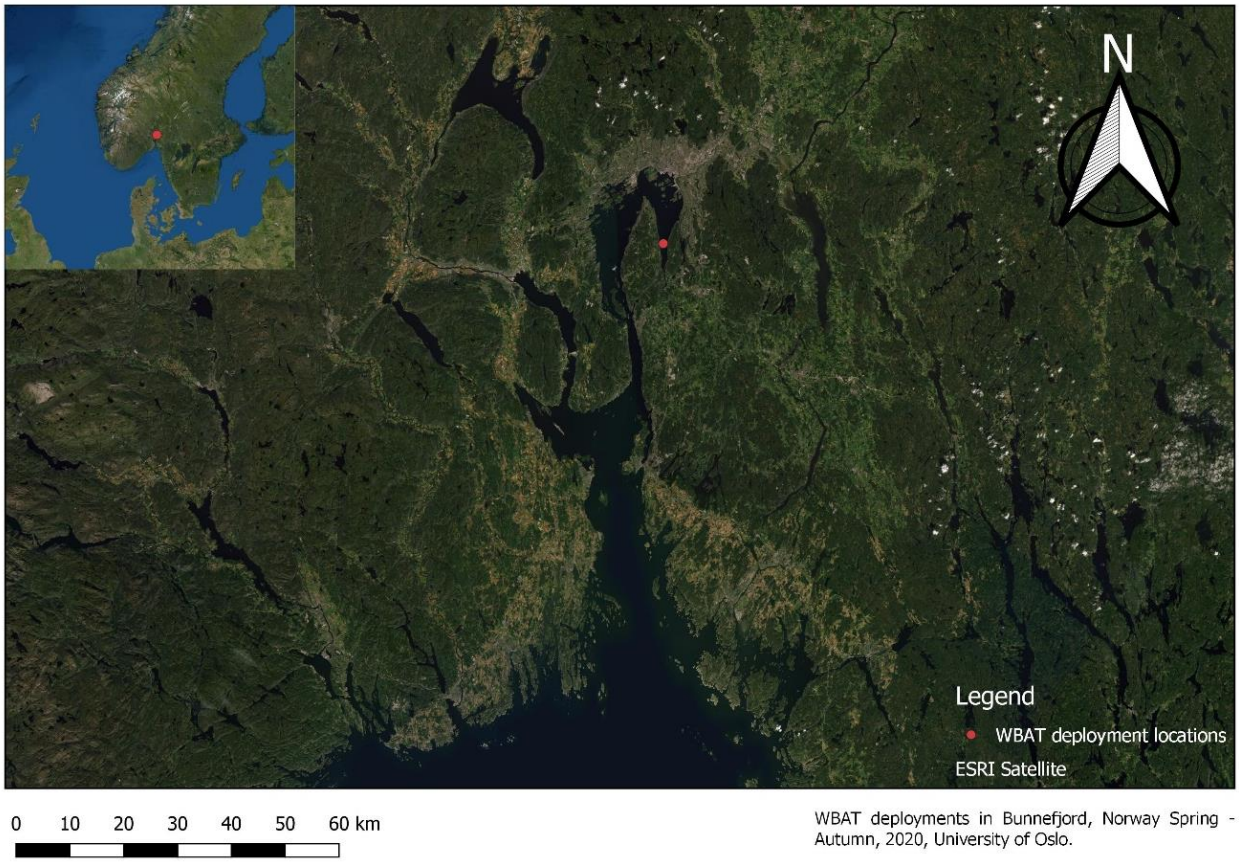

Fig. 2. Satellite image of the coastal inlet which ends in the inner Oslofjord, the Bunnefjord, where the WBAT echosounder was deployed during this study (red dot). Reference map of Scandinavia in top-left corner.

1.4 Acoustic Studies

DVM patterns can be observed through use of echosounders. Krill will appear as a layer on an echogram, called a sound scattering layer (SSL). Acoustic studies of krill can be done in different ways, either downward facing from a ship hull, or a submerged stationary upward facing echosounder. We did the latter, with a predetermined recording timeframe. Stationary equipment has been used previously to monitor DVM in euphausiids in temperate regions, on both west and east coastal Canada (De Robertis et al., 2003; Jaffe et al., 1999; Sato et al.,

2013; Sourisseau et al., 2008), as well as in the Oslofjord (Klevjer & Kaartvedt, 2011; Røstad & Kaartvedt, 2013; Vestheim et al., 2014).

It is also possible to use echosounders to study individual behaviors of organisms. By submerging an echosounder, a closer range to targets of interest helps resolving individual organisms, such as studies of krill in their daytime habitats. Acoustic studies of individual krill during daytime have previously been done in De Robertis et al. (2003), Jaffe et al. (1999), and Klevjer & Kaartvedt (2011). Because of the DVM patterns of krill, we can study individual krill behavior with a bottom-mounted echosounder during the day. According to Kaartvedt et al. (2009), *in situ* acoustic studies at depth are unintrusive for deep-living organisms.

1.5 Daytime Behavior of Krill

The main goal of this project was to investigate data collected from a submerged split-beam upwards-facing echosounder moored at the seabed in different seasons, spring to autumn. This was done in the Bunnefjord basin. The acoustic studies were supplemented with catch data from field sampling and environmental data. Our intent was to investigate population behaviors and individual behaviors at daytime when the scattering layer was close to the bottom. We also conducted some acoustic analyses on fish to address potential predator-prey interactions of krill.

2 Materials and Methods

2.1 Study area

Bunnefjord is the innermost part of the Oslo fjord system (Fig. 2). Waters here are to a less extent subject to exchange with outer coastal waters than other parts of the fjord due to being sheltered behind two sills (Klevjer & Kaartvedt, 2011). The outer sill in the Droebak sound is the shallowest at merely 19 meters. This lowers the rate of water exchange between both Vestfjord and Bunnefjord (which make up the inner Oslo fjord), with the coastal waters of Skagerrak (Klevjer & Kaartvedt, 2011; Rosenberg et al., 1987). The Bunnefjord basin's largest depth lies at approximately 150 meters, while the sill depth is 57 meters (Klevjer & Kaartvedt, 2011), which limits the water exchange even further. Conditions in the Bunnefjord become increasingly hypoxic over time, even excluding krill from the deep waters (Beyer, 1968; Kaartvedt et al., 2009). Yet, because of the limited water movement, Bunnefjorden is an ideal area for acoustic study of individual krill behavior when sufficiently oxygenated.

Data was collected on three locations in Bunnefjord, in its deepest part, slightly more than 150 m depth (Fig. 2, Fig. 3). These stations were at around 59°47.607'N, 010°43.127'E (Degrees Decimal minutes, DDM).

Fig. 3. Satellite imagery of Bunnefjorden. Locations (white dots) where the WBAT echosounder was deployed according to coordinates from field deployment data. Generated from plotting deployment coordinates (DDM) in QGIS.

2.2 Sampling Design

Sampling was done using an Isaac-Kidd midwater trawl (IKMT). On each sampling occasion, we used a ship-mounted echosounder onboard R/V Trygve Braarud, while moving through the fjord. This was a Simrad EK 500 (*Ocean Science Systems*, n.d.; *Simrad EK Series*, n.d.). This echosounder logged at frequencies 38 kHz and 120 kHz. Records from the hull mounted echosounders were used to select sampling depths. It identified an SSL visible at 120 kHz frequency but absent at 38 kHz (Fig. 4). This frequency response is typical for macroplankton like krill (Kaartvedt et al., 2005).

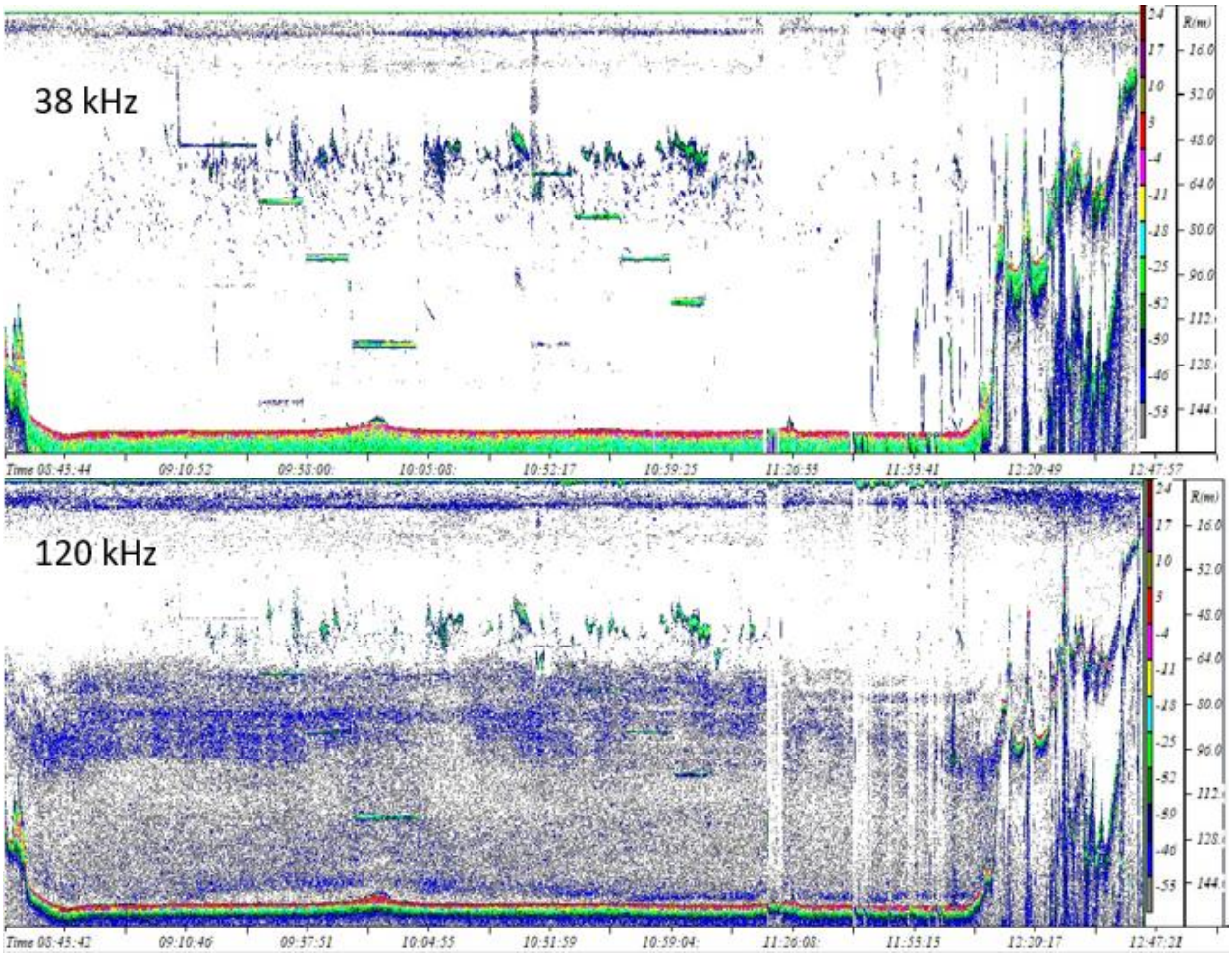

Fig. 4. Acoustic data from R/V Trygve Braarud hull mounted echosounder. Threshold -60 dB for both frequencies. Data from field campaign in August (06.08.2020). Stepwise echo traces are from sampling with the CTD. Color-bar gives the volume backscattering strength (S_v) in decibel, dB. R(m) is the range from the transducer, i.e., depth in this case. Echogram picture collected from Sonar5-Pro.

Sampling depths were selected based on this layer, normally with 5-6 depth intervals (Table 1), but also a few tows were done shallower than the layer, here used as controls. Trawl tows were conducted through roughly 15 minutes intervals at the sampling depth, supervised during sampling by means of a Simrad depth sensor. In the case of very large samples, the total catch would be measured by volume while a subsample of ~500 ml would be kept and frozen for later analyses. No biological sampling was done in March, due to Covid-19 restrictions. However, a CTD profile was obtained. Details on our sampling for both summer and autumn campaigning were as described in Table 1. The deeper parts of the water column were not sampled due to low backscatter in October. Due to small sizes, other plankton organisms such as arrow worms and copepods would not contribute significantly to the scattering strength we would later observe at 200 kHz (Sato et al., 2013; Trevorrow, 2005).

Table 1. Overview of field sampling in summer, and autumn.

August					**October**				
Trawl	Depth (m)	Time of day	Duration (min)	Catch	Trawl	Depth (m)	Time of day	Duration (min)	Catch
1 (control)	52	09:40 – 09:50	10	None (lion's mane and arrow worms)	1 (control)				None (comb jellyfish)
2	70	10:10 – 10:20	10	Krill	2	70	12:20 – 12:30	10	Krill
3	80	10:43 – 10:53	10	Krill and a few shrimp	3	90	13:10 – 13:28	18	Krill
4	90	11:16 – 11:26	10	Krill and one shrimp	4	115	14:10 – 14:25	15	Krill
5	100	12:29 – 12:39	10	Krill	5	130	14:50 – 15:07	17	Krill
6	120	13:16 – 13:21	15	Krill					
7	140	13:36 – 13:51	15	Krill					

2.3 Material Description

Acoustic data was collected using an autonomous 200 kHz WBAT echosounder (Kongsberg Maritime, n.d.). Predetermined programming enabled logging of acoustic data remotely, capable of being submerged for long time periods, as well as displaying high resolution down to individual level.

Data recording was done by deploying the echosounder at the seafloor mounted to a weighted rig. The WBAT was calibrated once in January 2021 (by research fellow Svenja Christiansen and PhD Beatrice Sobradillo) right beneath the surface during calm waters using a metallic calibration sphere following a standard setup according to the echosounder's documentation and as described in Foote et al. (1987). In analysis of individual behavior, we applied calibrated parameters to all data that was collected previously. For population analysis through >12 h echograms, factory settings were applied.

The Conductivity-Temperature-Depth (CTD) probe is a standard instrument for vertical profiling of important properties of seawater. This water profile is gathered from an instrument equipped with sensors that measure the conductivity, temperature, and depth in the surrounding seawater. This is useful because it describes changes in the environment that marine communities must cope with as depth increases. Conductivity provides a measure for salinity, and this together with temperature are driving determinants of water density. Typically, this is presented as changes in parameter unit with depth.

A CTD profile was obtained using a Sea-Bird, SBE 911 (Sea-Bird Scientific, n.d.), in spring. The instrument package was also equipped with a fluorometer. During summer and autumn campaigns this instrument was out of order. Thus, vertical environmental profiles were collected using an autonomous probe, SD204 (SAIV A/S, n.d.). This was slightly less precise, and provided temperature, salinity, pressure, and oxygen, but not fluorescence. The probe measured both on the way down the water column, and back upwards and sometimes provided noisy data. The probe's down- and upcasts had different oxygen profiles with lower values during ascent. The upcast profile has less precise readings oxygen readings in upper waters because of slow response, but more precise in the deep, which was more important for our purposes. We manually tidied the upcast data to a readable profile which provided the lowest oxygen value. The CTD data from March collected through Sea-Bird SBE 911 were uploaded to RStudio (RStudio Team, 2020), and analyzed using the 'oce' package (D. E. Kelley, 2018; D. Kelley & Richards, 2021). Environmental data gathered using SD204, was directly analyzed using base R functions (R Core Team, 2019).

2.4 Field campaigns

Field excursions would generally span 3-4 days with UiO research vessel, R/V Trygve Braarud. The first day would usually be spent on handling and deployment of the WBAT echosounder. Setup of the echosounder was done by Svenja Christiansen, and later mounting to rig and deployment in the water would be executed by the ship's crew (Fig. 5A). The remaining excursion time would be consisting of collecting other hydrographic and environmental data such as CTD, fluorescence, and collection of biological samples (Fig. 5B). When retrieving the WBAT echosounder, the data was transferred to a hard drive before either being redeployed immediately for future recording or stored in a warehouse at the docks.

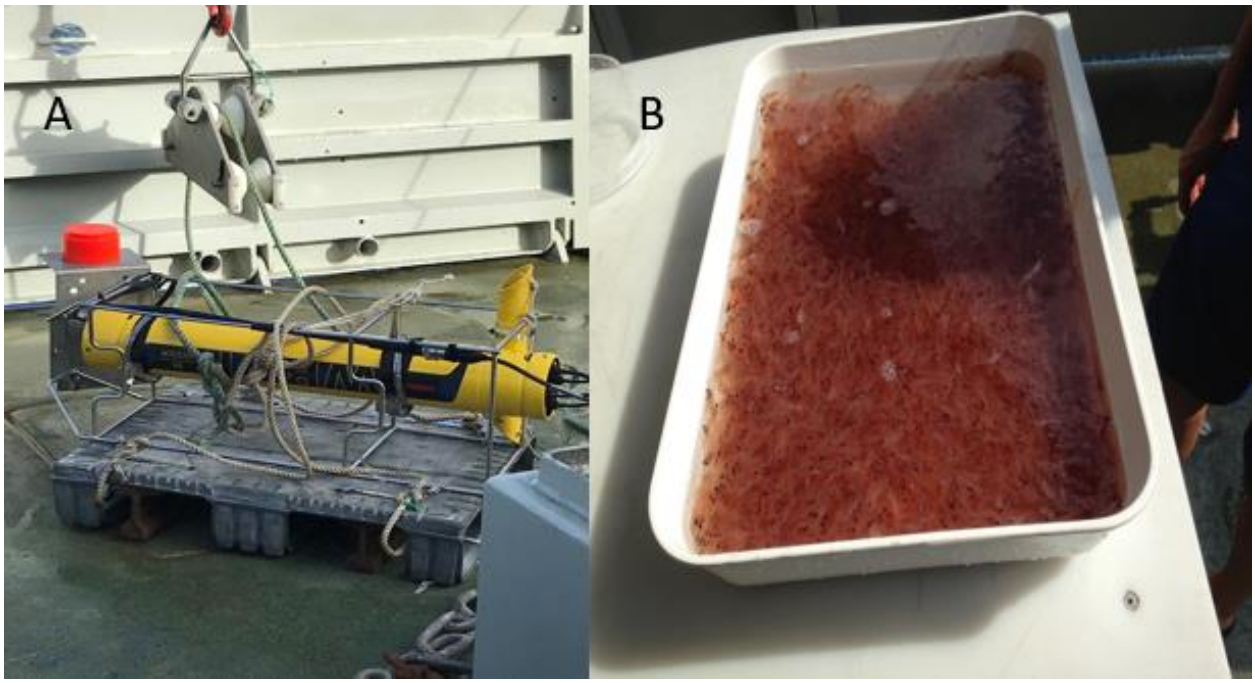

Fig. 5. A: The WBAT echosounder as it would appear when mounted to a weighted rig for seabed deployment. [Photo: F. L. Moksnes]. B: Catch from biological sampling using an IKMT. In this photograph, the catch was dominated by krill [Photo: S. Kaartvedt].

2.5 Post-processing

Data files logged in the echosounders' memory was stored on external drives, and converted from raw files to calibrated data by applying calibration parameters obtained from the standard calibration procedure (Foote, 1987). For visual analysis, these files were merged to produce continuous echograms, enabling visualization of a time-lapse of each logged file, which alone amounted to ~15 minutes of recorded data. This way, longer time frames can be visualized. For example, a 24-hour period, or several days and nights. This was done using Sonar5-Pro (version 606.22) which is a software developed for analysis of acoustic data, by the Institute of Physics at UiO (Balk, 2021). At greater depths organisms have a greater resolution and swimming patterns become clearly visible as they are closer to the echosounder's transducer, which is advantageous as it helps to reduce uncertainties related to unclear tracks far away from the acoustic beam (Christiansen et al., 2019).

2.5.1 Population analysis

Population behavior was analyzed in Sonar5-Pro and visualized in RStudio (RStudio Team, 2020). For visualization, the uncalibrated raw data was processed into gridded data

beforehand, which was based on echosounder factory defaults. This was done by Doctoral research fellow Svenja Christiansen. The raw volume backscatter strength (S_v, in units of decibels, dB) data was gridded into 0.001 days (i.e., 1.44 min) and 0.25 m intervals. This procedure enables large-scale pattern visualization of backscatter over depth and time. The S_v value of each grid cell was then determined by calculating the average of all S_v values that was found within each respective depth and time interval in the linear domain. This created a compressed dataset suitable for working with in RStudio (RStudio Team, 2020). Generating echograms in RStudio was done using R packages 'fields' and 'ncdf4', and base functions (Nychka et al., 2017; Pierce, 2019; R Core Team, 2019).

Population analysis was done by using an AMP echogram which outputs all data that is recorded and displays backscatter. We started to assess individuals by narrowing down to smaller vertical range intervals and timeframes, to observe individual behavior, displayed as echo traces.

2.5.2 Individual analysis

Individual analyses were assessed in Sonar5-Pro (Balk, 2021). Individual analyses were done by zooming in on smaller timescale of temporal patterns observed in the daytime depth of the scattering layer and subjectively selecting echo traces, as it is possible to view individual tracks clearly close to the transducer. Finer scale echograms were visualized by exporting sample data from Sonar5-Pro into RStudio.

We also observed individuals through target tracking (TT) (Balk, 2021). TT is enabled using an SED echogram, which differs from AMP echogram by having a set of strict criteria that must be fulfilled for registering sequential echoes as an echo track. The SED echogram use an algorithm to filter out echoes that don't fulfill its requirements rejecting those not belonging to a single organism (Kaartvedt et al., 2009). This way, sequential echoes is most likely the track of one organism in the beam. TT is best conducted in within limited range interval as very close tracks don't yield meaningful results and far away targets are too many to resolve because of the expanding cone shape of the beam (Kaartvedt et al., 2009). By using a split-beam echosounder we could collect data on an organism's orientation in four quadrants, making it possible to observe its movement in the horizontal plane of the echosounder beam in addition to its placement in the water column (Simmonds & MacLennan, 2006). This enabled us to visualize the track data in three dimensions.

In our study this was applied to observe swimming patterns, similar to what some previous research has demonstrated (Klevjer & Kaartvedt, 2003, 2006). Our aim was to exemplify the swimming patterns individuals display in late March. Christiansen et al. (2019) was consulted for parameter settings for the target tracking.

Using tracking data from Sonar5-Pro enabled us to visualize swimming patterns of selected individual krill. Three-dimensional models of swimming patterns was plotted using RStudio (R Core Team, 2019; RStudio Team, 2020), with package 'plotly' (Sievert, 2020).

2.5.3 Supplemental data

DVM timing in krill may be influenced by varying daylengths (Sato et al., 2013). We retrieved solar periods to assess seasonal DVM changes in relation to daytime. Acoustic data is recorded in Greenwich Meridian Time. Hence times for local sunrise and sunset in UTC were collected using a sunrise.set function in R package 'StreamMetabolism', which is based on NOAA's sunrise/sunset calculator (Sefick Jr., 2016; US Department of Commerce, n.d.). We used coordinates for the echosounder (Fig. 3). These times where again checked and verified by comparing with weather data from timeanddate.com (*Sunrise and Sunset Times in Oslo, August 2020*, n.d.; *Sunrise and Sunset Times in Oslo, March 2020*, n.d.; *Sunrise and Sunset Times in Oslo, October 2020*, n.d.).

Maps and satellite imagery of the study area were generated using open-source mapping software QGIS (QGIS Development Team, 2021). Here we used the QuickMap Services plugin which enabled using ESRI Satellite images as map layers when plotting our station coordinates. The procedure for this was found in Erazo (2018).

2.6 Laboratory procedures

Measurements

Length measurements of krill were done following procedures listed in Hassel et al. (2013). Length measurements are usually based on the krill's total length, which means distance between the apical end of their rostrum to the tip of the telson. However, breakage of the rostrum during sampling occurred frequently, something that we observed as well (Hassel et al., 2013). Thus, total length was measured from the front of the eyes to the tip of the telson. Length measures were carried out by aligning krill fully stretched out next to a ruler or on millimeter paper. A random subsample of 50 individuals per sample was measured. A sample from an IKMT can be quite large, causing counts of individuals time consuming. In these instances, rough number of individuals was estimated through measuring volume (Fig. 6). For example, by measuring the volume of 100 krill as well as the volume of the entire sample enabled us to simply compute a rough estimate of the total number of individuals in the entire sample. Plotting results was done in RStudio using 'ggplot2' (Wickham, 2016).

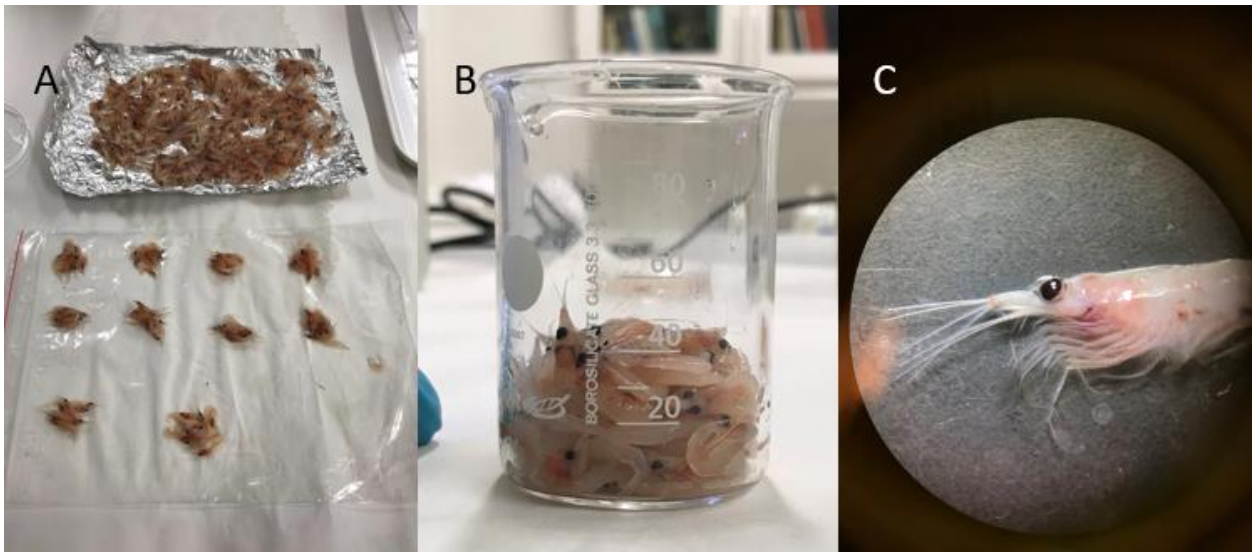

Fig. 6. Some pictures from the lab. A: After thawing samples, krill were counted, and a subsample was measured (not shown here). B: Counts estimated through volume, here measured in a beaker. C: *M. norvegica* through a magnifying glass. [Photo: F. L. Moksnes].

Stomach investigations

We checked whether krill had preyed on smaller animals in our samples by dissecting and physically inspected stomach content under a microscope. The stomach lies on the dorsal side of the body right behind the eyes, almost at the segment margins. It is almost conical in shape; thus, the structure is easily identified, and isolated physically using forceps (Fig. 7A). It was further dissected by cutting it in to as small fragments as possible using a scalpel directly on an object glass. When observing the gut content under the microscope, we checked for remains of calanoid mandibles as these remain mostly intact in comparison to other digestible organic matter and are easily identifiable (Fig. 7B). In most instances identification down to species level can be done and has repeatedly been used as a target in studies of gut contents in krill (Barange et al., 1991; Gibbons, Barange, et al., 1991; Gibbons, Pillar, et al., 1991; Karlson & Båmstedt, 1994; Stuart & Pillar, 1990). However, species identification of copepods by investigating mandibles through microscopy was beyond the scope of this project.

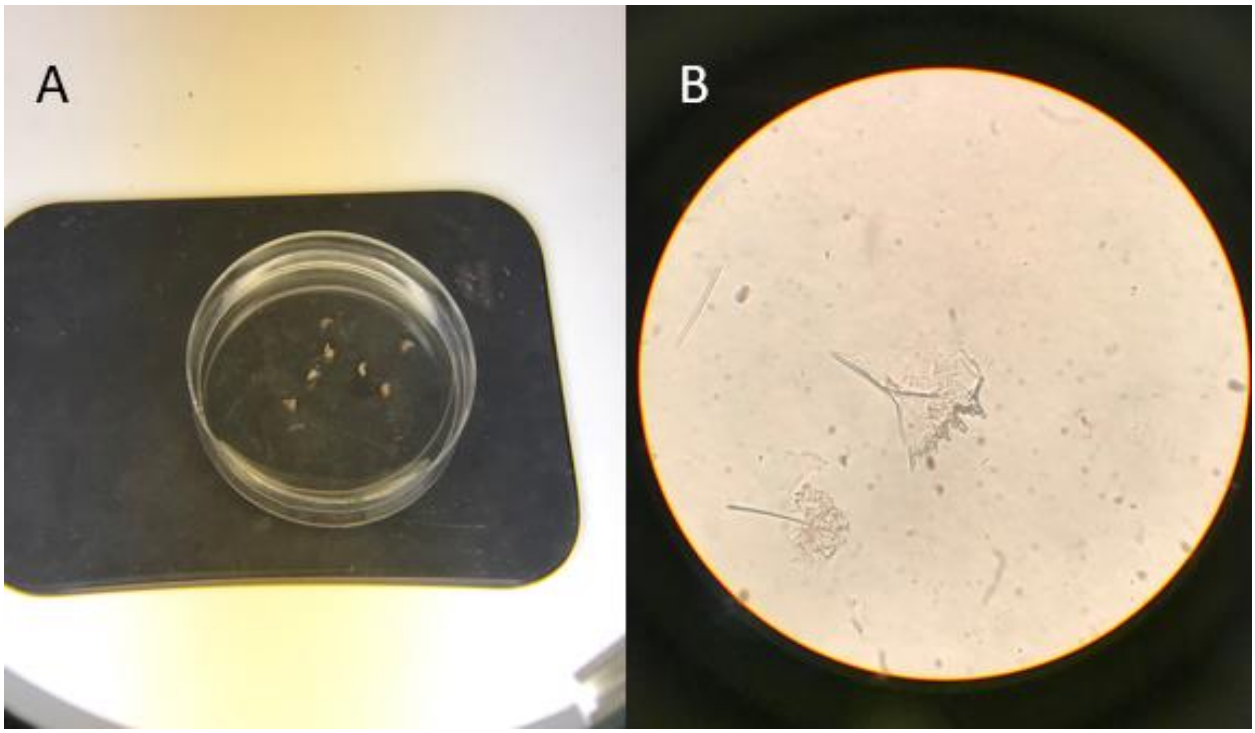

Fig. 7. A: Exctracted stomaches of *M. norvegica*. B: Calanoid mandible found in a krill gut, captured through light microscopy lens. [Photo: F. L. Moksnes]

3 Results

3.1 Environment

3.1.1 March

Salinity was <26 PSU at the surface, steeply increasing to ~31 PSU at 20 m, and reached a maximum salinity of ~33 PSU at ~60 m towards the bottom (Fig. 8).

Temperature increased from surface level temperatures at ~4℃ to a warm core at ~20 – 40 m depth until a maximum temperature of ~9.4 ℃ at around 40 m depth. From here, the temperature declined until reaching a stabilization at ~60 m with a temperature of ~8.1 ℃ from where it slightly increased towards the ending ~8.4 ℃ in bottom depths (Fig. 8).

Oxygen fell from ~8.5 mg/l at the surface down to 20 m where it was ~2.5 mg/l. Here, O_2 levels remain stable for about 40 meters. Below 60 m the oxygen concentrations declined again, although more slowly than the previous depth interval ending below 2 mg/l towards the seabed.

Fluorescence given in arbitrary units, rapidly increased between ~4 m. and ~10 m depth where it reached a maximum point. From here fluorescence declined rapidly until a minimum, from where it increased again below ~40 m. From here it steadily increased towards the seabed where fluorescence was about 2/3 of the maximum values that was observed in the upper layers (Fig. 8).

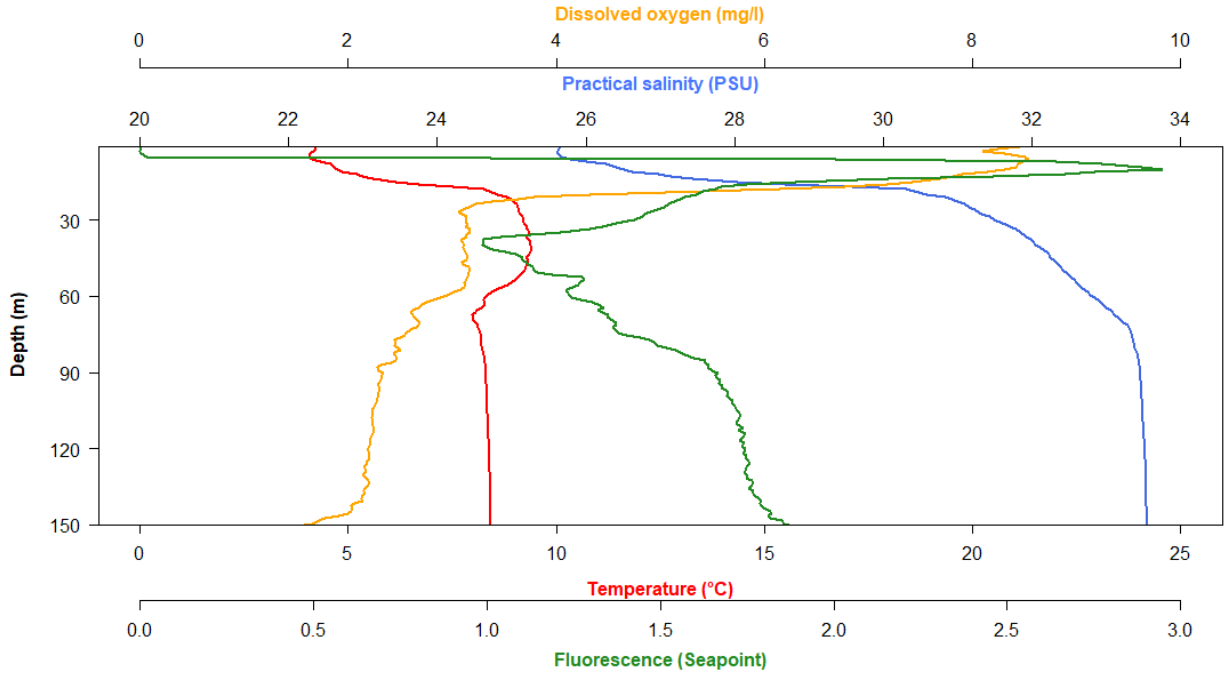

Fig. 8. Vertical environmental profiles (CTD) using SeaBird SBE 911. From March field campaign (09.03.2020). Colored graphs to match their colored descriptions on axes for ease of reading.

3.1.2 August

In the summer salinity was <20 PSU near the surface, rapidly increasing to ~30 PSU in the upper 20 m, before flattening out at ~33 PSU at ~60 m and to the bottom (Fig. 9).

Temperature was ~20 ℃ at the surface, and quickly reduced to ~10 ℃ at 20 m. At this depth, the decline in temperature flattened out and stabilized at ~65 m where the temperature remained at about 8.3 ℃ the entire way down to the seabed (Fig. 9).

Dissolved oxygen had a concentration of 8.3 mg/l near the surface and rapidly declined to ~3 mg/l at 20 m before rising again. The intermediate increase in oxygen concentration lasted for ~20 meters peaking at ~43 m depth, to a concentration of ~4 mg/l. Below this point, oxygen levels had yet another steep decline down to ~60 m with a concentration of ~2.5 mg/l. Decline slowed down and was at this point ~2 mg/l at 80 m. From here the oxygen profile remained stable down to 120 m. Below 120 m, oxygen levels declined below 2 mg/l, coming down to about 1,2 mg/l at ~146 m (Fig. 9).

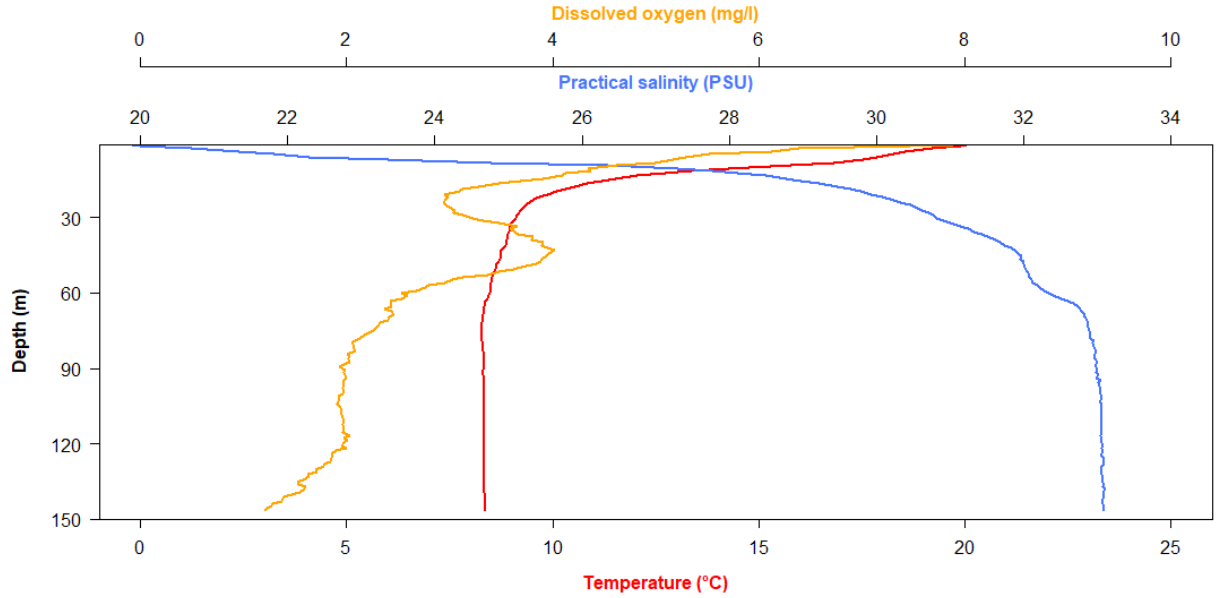

Fig. 9. Vertical environment (CTD) profile of Bunnefjord during August field recording (06.08.2020). Based on upcast data gathered through use of autonomous probe.

3.1.3 October

In autumn, the temperature profile was like August except for cooler surface water. Similar in that we observed a rapid decline in temperature down to 20 m. Below 20 m, we observed the temperature's curve flattening out and stabilizing at a minimum temperature around 8.3°C below 60-70 m. depth (Fig. 10).

Salinity was ~25 PSU in the near-surface waters and increased to 30 PSU at 20 m. From here it flattened out with the slope stabilized at 33 PSU at ~70 m and towards the seabed (Fig. 10).

The shape of the oxygen profile was similar between August and October, but with lower values in October and were close to zero in the deepest part of the water column (Fig. 10). Surface level concentration held ~7 mg/l, and quickly reduced to ~2,6 mg/l at 20 m. After this, the oxygen concentration a slightly increased towards 50 m where it peaked at ~3 mg/l, a similar pattern as in August although at greater depth. Below 50 m oxygen declined rapidly towards 60 m (<2 mg/l) where the curve flattened out, steadily declining the entire way down to the seabed, reaching a minimum concentration of less than 0.01 mg/l (upcast value) (Fig. 10). The lowest downcast value fluctuated between ~0.7 and 0.07 mg/l at the lowest depth recordings for the duration of an acclimatization period at the maximum recording depth. This

gave us an uncertainty of about 0.06 mg/l i.e., a range between <0.01 and 0.07 mg/l to be expected from our recordings.

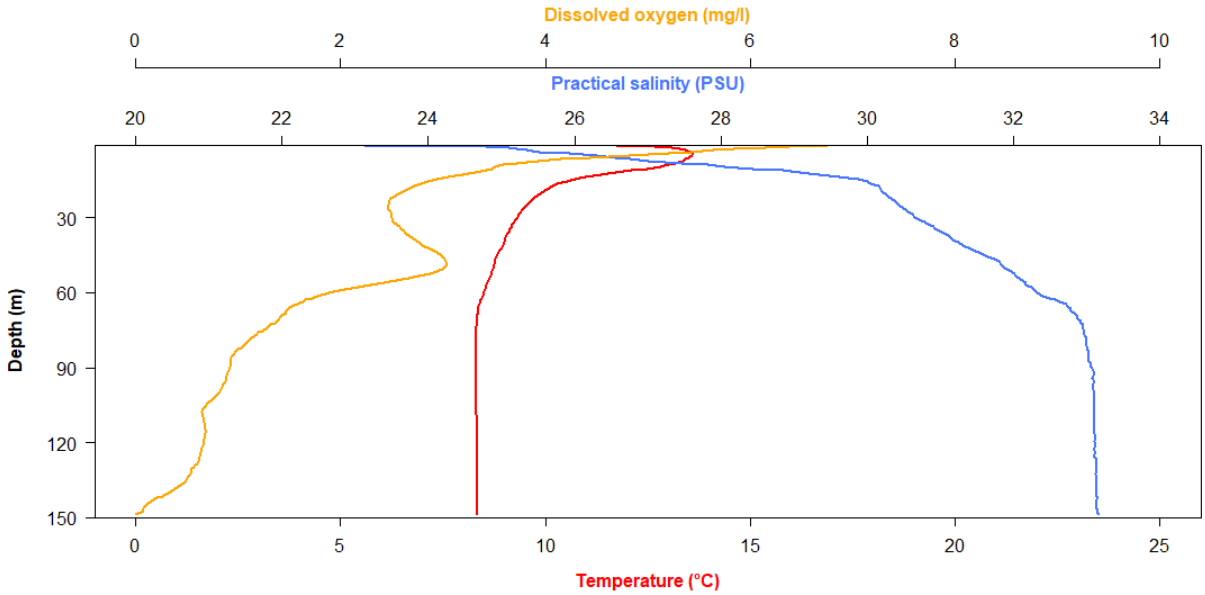

Fig. 10 October's CTD profile (20.10.2020). Coloration of graphs are to match coloration of parameters. Data presented were based on the upcast.

3.2 Catch Data

3.2.1 August

Catches in August yielded large volumes of krill and some pelagic shrimp of genus *Pasipahea* (<1% of numbers, and only present at 80 and 90 m). The numbers increased by depth, with a slight decrease in the deepest interval (Fig. 11).

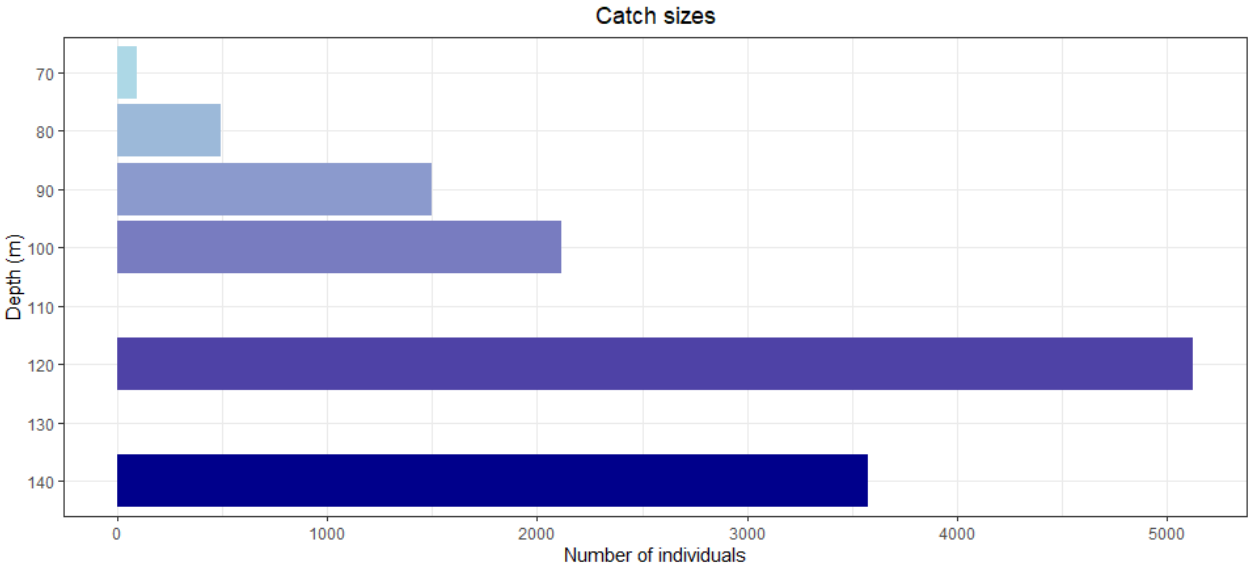

Fig. 11. Estimated total catch sizes collected from IKMTs in August. Data based on the estimated total catches by volume. Colors are used to visualize increasing depth, from light to dark. Control sample at 52 m yielded no krill, data not shown.

Size distribution (measured in total length, TL, Fig. 12) varied by depth (ANOVA: $p<0.05$), length measured from each sampling depth yielded larger individuals in the shallows. Averages in krill size ranged between 33.44 ± 2.28 mm, and 31.14 ± 2.94 mm (Fig. 12).

Pairwise comparisons between sampling depths using t-tests showed significant variation between 70 m and 90 m, 70 and 100 m, 70 and 120 m, 70 and 140 m, 80 and 90 m, 80 and 100 m, 80 and 120 m, and 80 and 140 m depth. As Fig. 14 demonstrates, the size variation is most noticeable between the upper krill layer of 70 – 80 m and samples from 90 – 140 m.

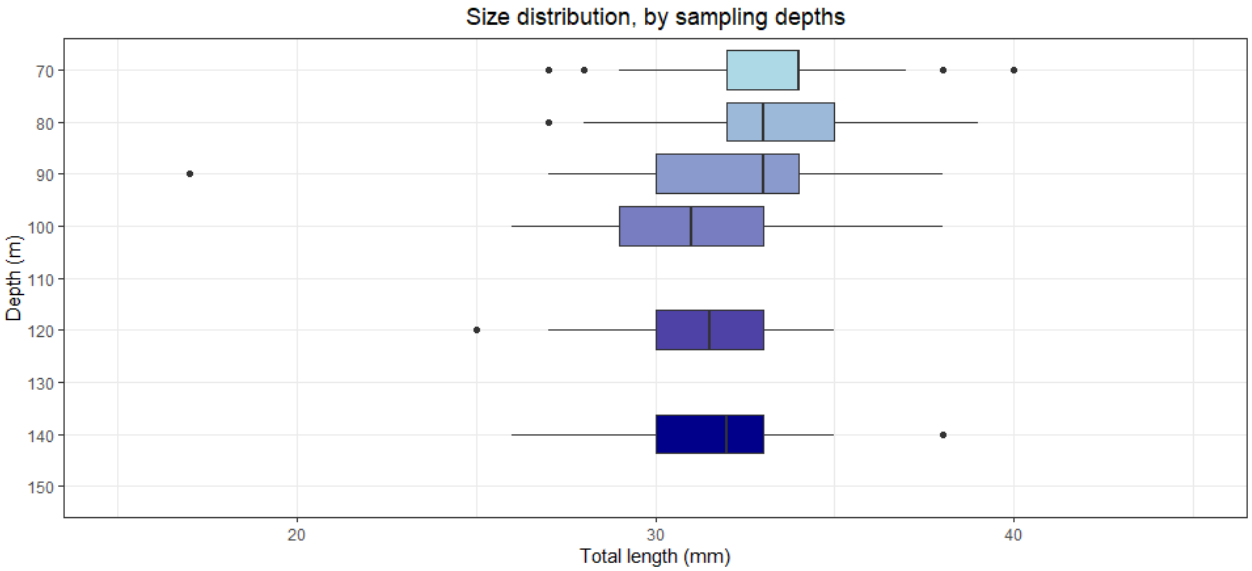

Fig. 12. Size distributions by depth. Sizes as total length (TL) in sampled krill. Sizes were based on a subsample of 50 individuals randomly selected from each sample, 300 individuals in total. Colors visualize increasing depth.

3.2.2 October

In October fewer trawls were conducted, yielding 4 samples (depths) in total. In this case, catches were larger in shallower depths (Fig. 13) and subsequently decreased in size further down the water column (Fig. 14).

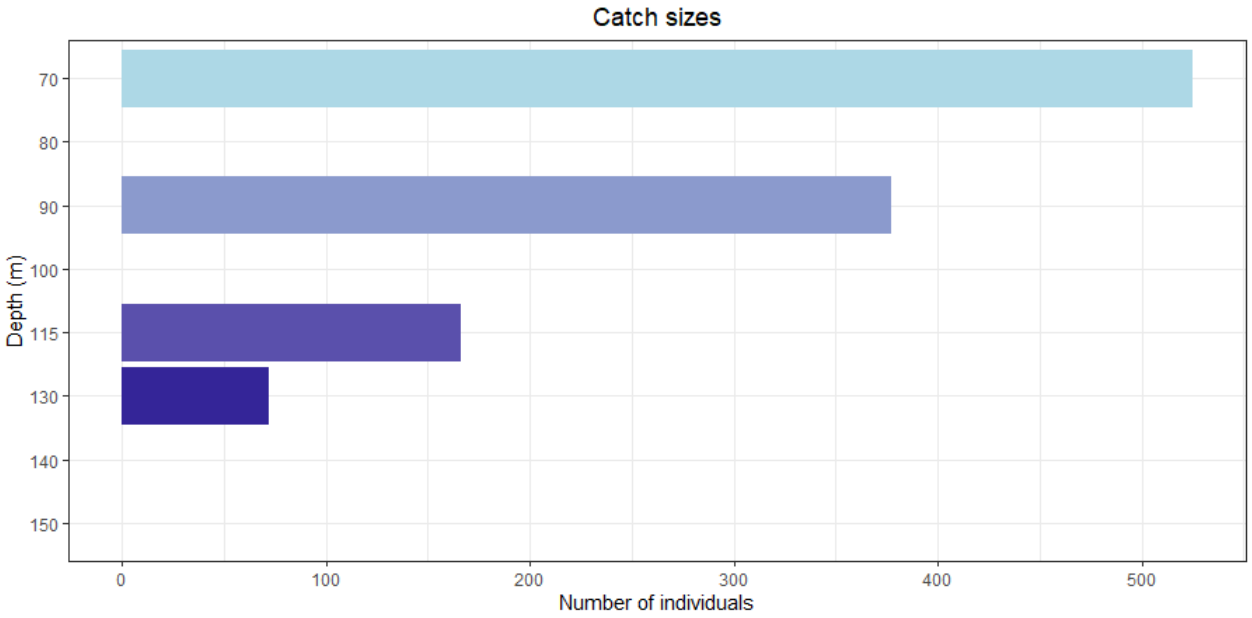

Fig. 13. Catches from IKMTs in October field campaign, 20.10.2020. Numbers were based on the estimated total catches by volume from each sampling depth. A control sample at ~30 m yielded no krill, data not shown.

Average sizes (TL) in October catch data ranged between 30.28 ± 2.92 mm, and 32.57 ± 2.60 mm (Fig. 14).

October size testing also showed significant variance in size between depths (ANOVA: $p < 0,05$). Pairwise t-tests comparing depths showed significant difference between 70 and 90 m, 90 and 115 m, and 90 and 130 m.

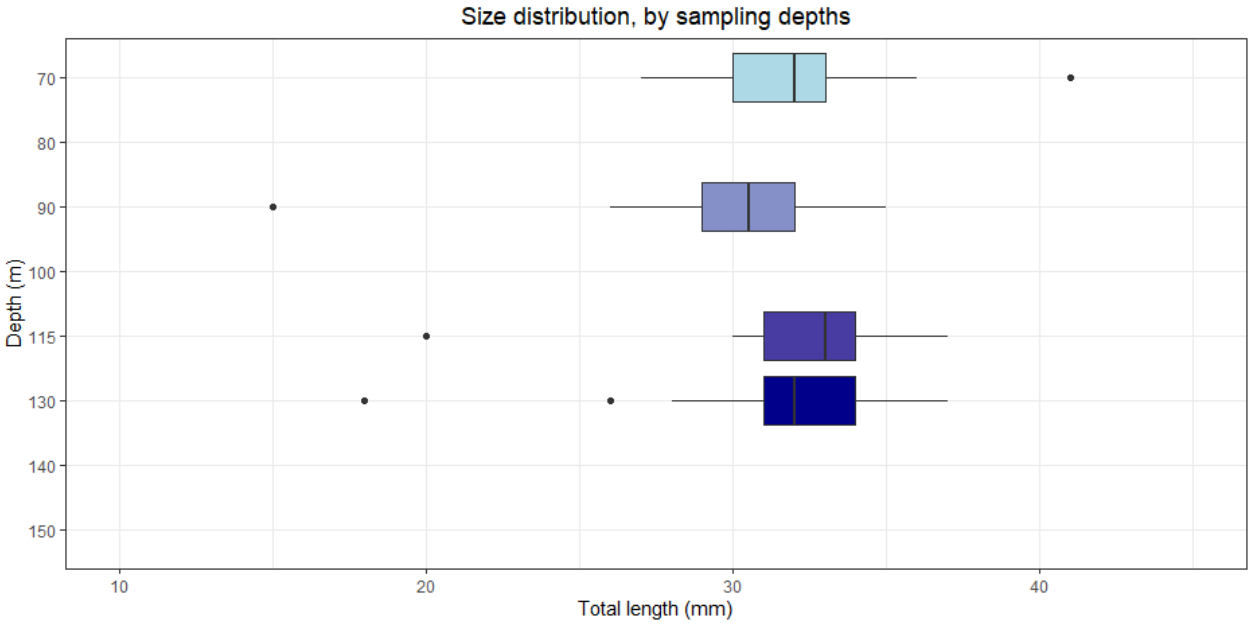

Fig. 14. Size distribution of krill caught in October campaign. N = 50 individuals each case (except for 130 m, where entire sample of 72 krill was counted and measured).

3.2.3 Stomach investigations

August samples yielded most mandibles in the deepest waters, but mandibles were present in all samples (Fig. 15). Stomach investigations from biological samples in October yielded only a few mandibles in ¾ of the samples, with 3 and 4 mandibles in the upper waters, at 70 and 90 m respectively. Only 1 mandible was observed below this. Because of the few observations, October samples were not analyzed further.

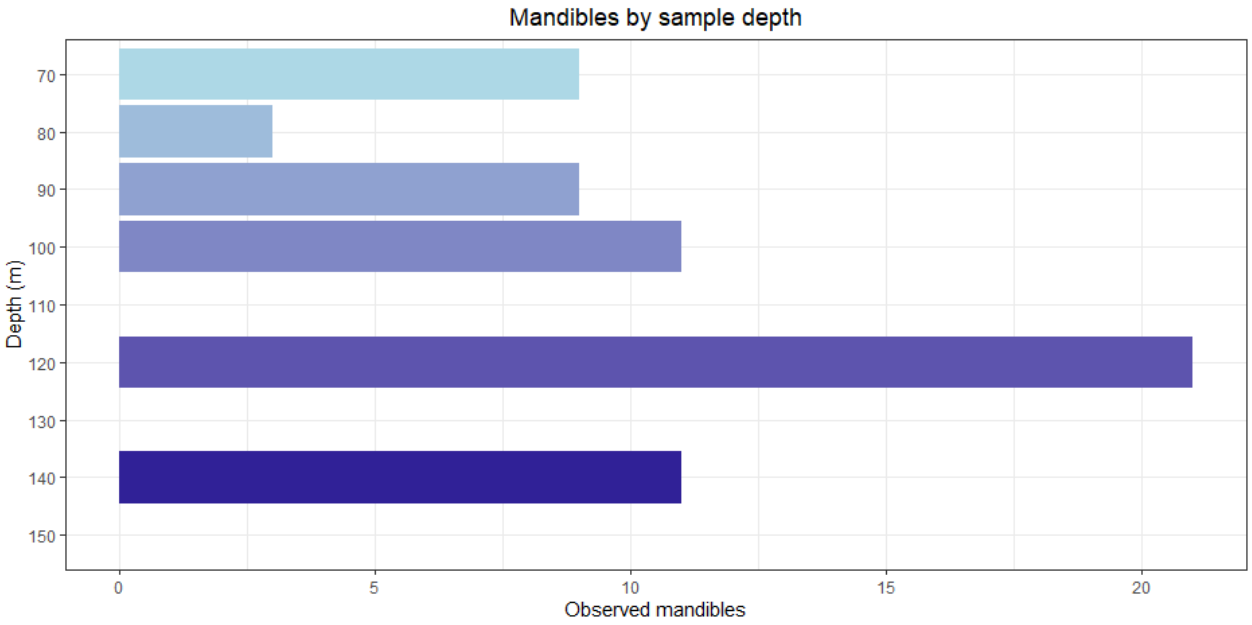

Fig. 15. Mandibles from August samples (11.08.2020). Most mandibles were observed in samples from deepest waters. Data presented based on n = 10 krill stomachs per sample, 60 total.

3.3 Acoustic Data

3.3.1 March

Population analysis

The SSL carried out DVM throughout the entire recording period, with little variation between days (Fig. 16A). A slight variation in daytime depth distribution occurred towards the end of the campaign period, but in general the entire population migrated in a similar fashion throughout, up at night and down by daybreak. There was some change in the daytime distribution, the deepest was at noon where it spanned from ~70 m down to ~130 m i.e., the krill layer had a vertical range of about 60 m around noon. A shallow layer of strong backscatter was observed above the krill layer and followed it during migrations, but generally remained above it.

The evening ascent to shallower waters started ~1 - 2 hours before the estimated time of sunset and accelerated after. The SSL reached the shallows at approximately 1 hour after sunset (~17:45). The population migrated to a depth of ~14 m (the echosounder was deployed at a depth of 154 m). Here, the population aggregated to a high vertical density i.e., a narrower vertical range compared the SSL's distribution during daytime.

Scaling down to a 24 h perspective showed that there were sinking echo traces outside of the SSL core during daytime, after the dawn descent, and before dusk ascent (Fig. 16B). This behavior was most noticeable deeper in the water column, from ~90-100 m down to the bottom. We did not observe a second aggregation of krill at the seabed although they were observed to sink down to it, thus they did not stay at these depths and must have returned upwards back to the general SSL distribution range. Sinking behavior was documented, even at periods of dusk ascent when the entire population generally migrated upwards (Fig. 16C).

Following the termination of upwards ascent in the evening there was a short period where the entire population was densely aggregated between 5 and 15 m depth. However, the entire krill layer did not remain at this level for long. We observed shortly after that this period was followed by re-formation of a gradually deepening layer after 19:00. The backscattering strength of the core in the shallows fades after 22:00, and the vertical distribution of the layer

was at this point observed from surface level down to 70 m. The scattering layer would remain like this until the time of descent (Fig. 16B and C).

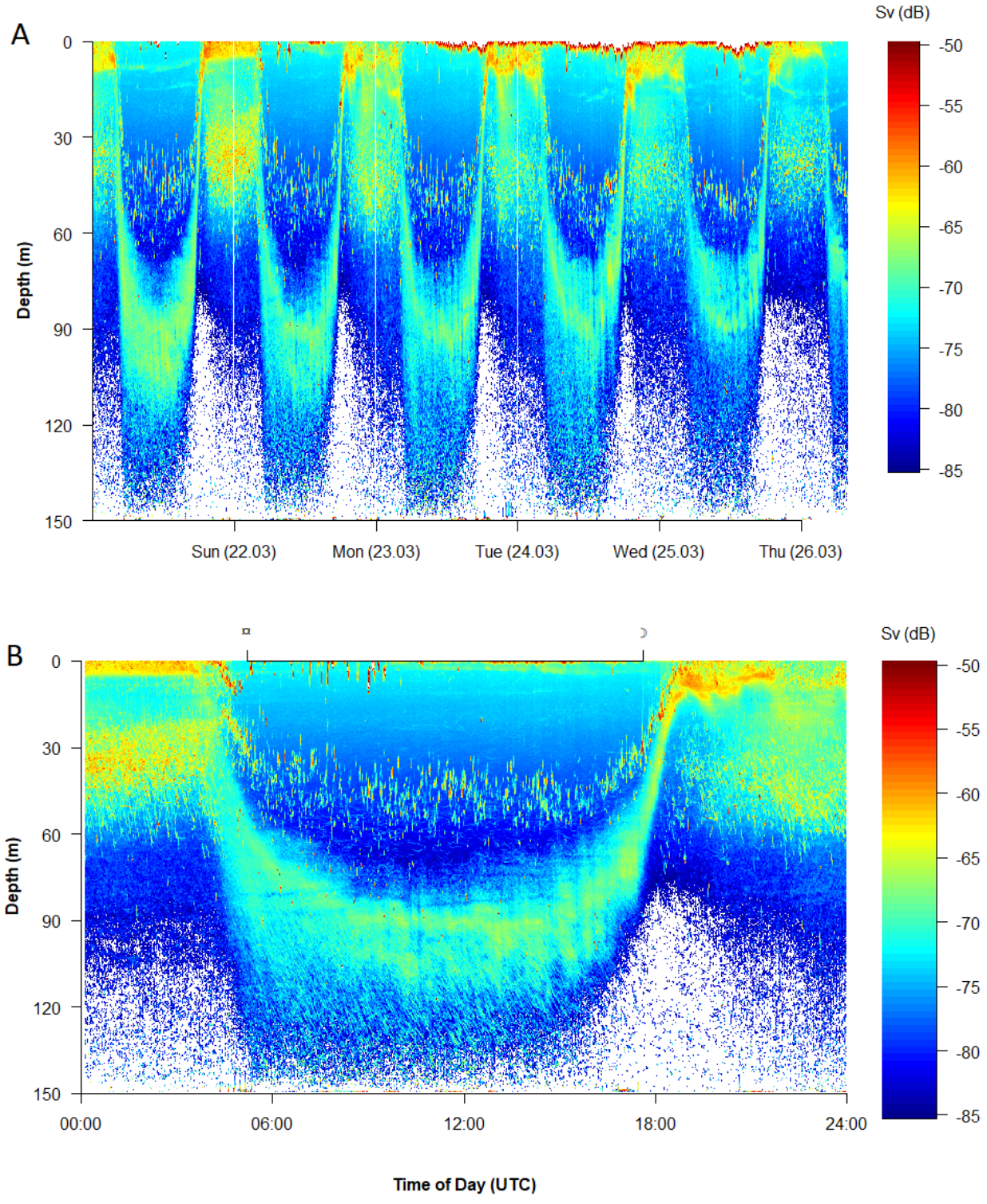
A
Sv (dB)
-50
-55
-60
-65
-70
-75
-80
-85
Depth (m)
0
30
60
90
120
150
Sun (22.03)
Mon (23.03)
Tue (24.03)
Wed (25.03)
Thu (26.03)
B
Sv (dB)
-50
-55
-60
-65
-70
-75
-80
-85
Depth (m)
0
30
60
90
120
150
00:00
06:00
12:00
18:00
24:00
Time of Day (UTC)

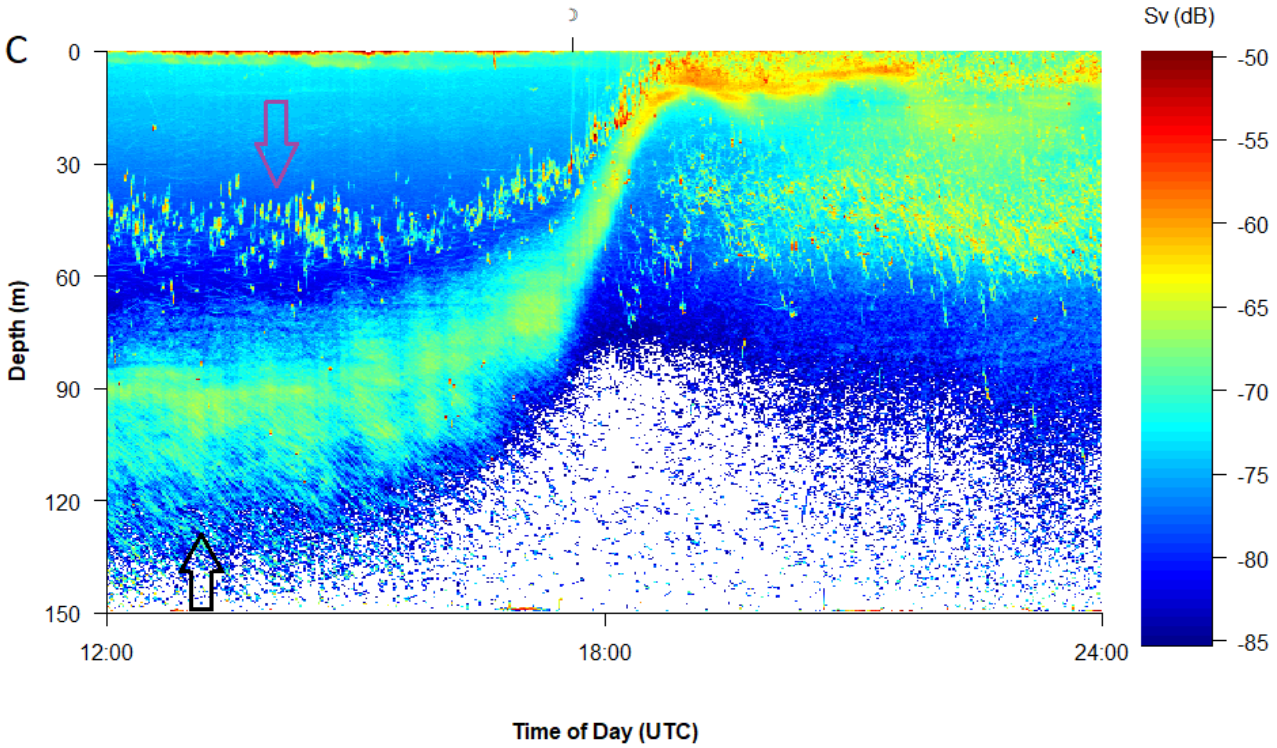

Fig. 16. Acoustic data from March. Thresholds were set between -85 and -50 dB. Vertical axis provide depth, and volume backscattering strength (S_v) provided in legend color strip. The horizontal axis provides the days of recording. Time of sunrise was calculated to be around 05:00 and sunset at 17:30 – 17:50 (UTC) in March and marked with sun (☼) and crescent moon (☽) symbols. The center of the scattering layer, where the backscatter is stronger, exceeding -60 dB, indicates high densities, or large organisms, referred to as the core of the layer. A: March recording days summary, 21.03.2020 – 26.03.2020. B: Echogram displaying scattering layers through a 24-hour period (22.03.2020), from midnight to midnight. C: Half of a day's recording (on 22.03.2020), displayed from noon to midnight in March. This presentation highlights the transitioning period between daytime distribution and the nighttime distribution, a dusk ascent. Time of sunset is marked with crescent moon (☽) Black arrow highlights sinking traces in deep waters. Purple arrow highlights a shallow layer with high backscatter that followed the krill layer, further assessed on p. 38.

Individual behavior analyses

Exploring the example portrayed in Fig. 16 on finer scale, we zoomed in on individual echo traces and their patterns throughout the daytime. We observed clear sinking patterns closer to the transducer during the day, most noticeable outside of the core of the scattering layer where organisms appeared too dense to filter out single tracks. Fig. 17 displays individual sinking tracks closer to the seabed i.e., closer to the transducer beam. Such behavior was observed throughout the recording period in March. Some weaker targets were recorded as krill returned and swam upwards.

Most of the individual sinking behavior down from the SSL was observed during daytime. However, we observed also that there were some individuals that are sinking while the SSL was moving upwards.

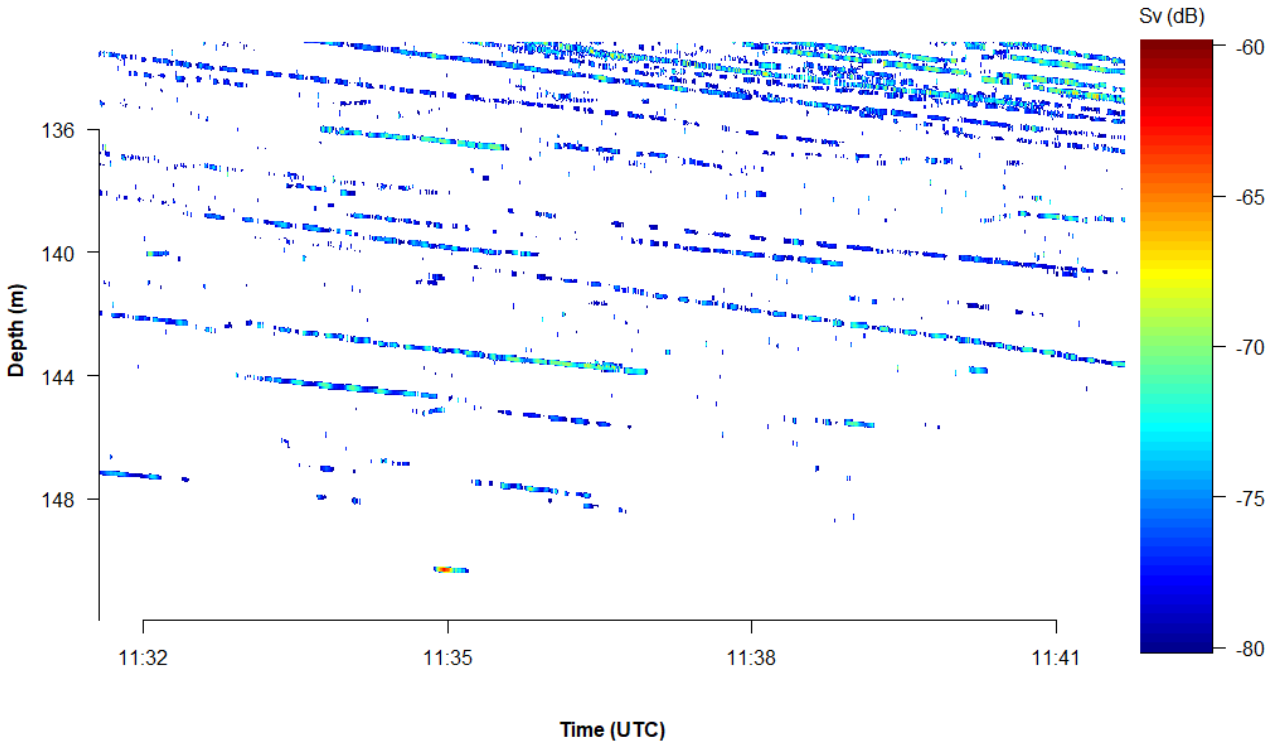

Fig. 17. Example of daytime sinking individuals in deep waters. Picture collected from zooming on ranges most close to the transducer and a -80 dB lower threshold. Record from 22.03.2020.

After the initiation of the dusk ascent (Fig. 16), it was still possible to observe sinking traces higher up the water column outside of the SSL. There were more individuals moving in an upwards oriented fashion, but some were still sinking. Fig. 19 provides an example of the

deepest edge of the SSL slightly higher up the water column during the event of dusk ascent. On longer ranges the traces became weaker and more distorted.

Manually measured individual traces had an average sinking velocity of 6.84±1.33 mm·s^{-1} (n = 15). There were no variations between days or the time of day (Table 2, ANOVA: $p>0.05$). Even though we could not resolve individuals in the krill layer, we observed traces there to be parallel with the individuals closer to the transducer that we could resolve. Thus, we assumed similar velocities occurred here as well. More details on daytime sinking individuals in March are listed the appendix (Table B 1). Where we could observe faint traces turn and swim upwards, we found an average swimming speed of 21 ± 3.5 mm·s^{-1} (n = 20).

Table 2. Average sinking speeds (millimeters per second) as from krill echo traces physically measured. Depths were between ~110 and ~140 m. further up the water column traces where too close to the SSL core to be individually resolved. N = 15 traces, 5 for each case.

Part of daytime (hours)	**Morning (08-11)**	**Noon (12)**	**Afternoon (14-17)**
Mean velocity (mm·s^{-1})	7.34	6.99	6.19
Standard deviation (mm·s^{-1})	1.03	1.87	0.90

Acoustic target tracking was used to assess 3D behavior of sinking patterns in the daytime. Typically, krill would sink in a spiraling fashion, as demonstrated in Fig. 18. Because of their closeness to the transducer, data were in high resolution and data smoothing was not necessary. The circles created in the spiraling behavior was observed to be ~0.10 – 0.20 m wide (Fig. 18).

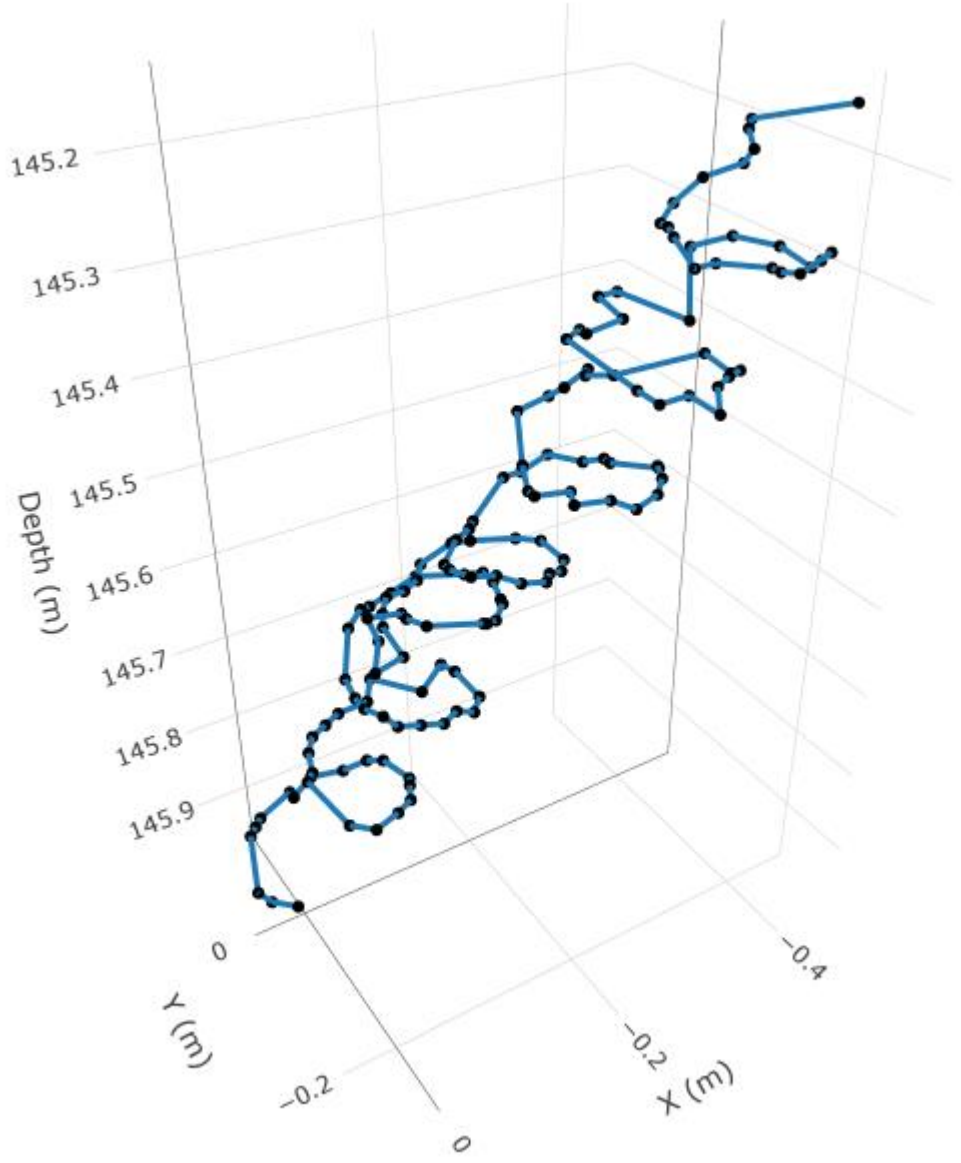

Fig. 18. 3D Sinking pattern in from a single track moving for <2 minutes. Captured on 22.03.2020 at around noon ~8-9 meters from the echosounder transducer. X and Y coordinates are positionings in the horizontal plane.

Although the general behavior in March was sinking from the SSL, it was not the only type of behavior observed. Later in afternoon we observed another type of behavior where traces displayed a sink and return upwards pattern (Fig. 19).

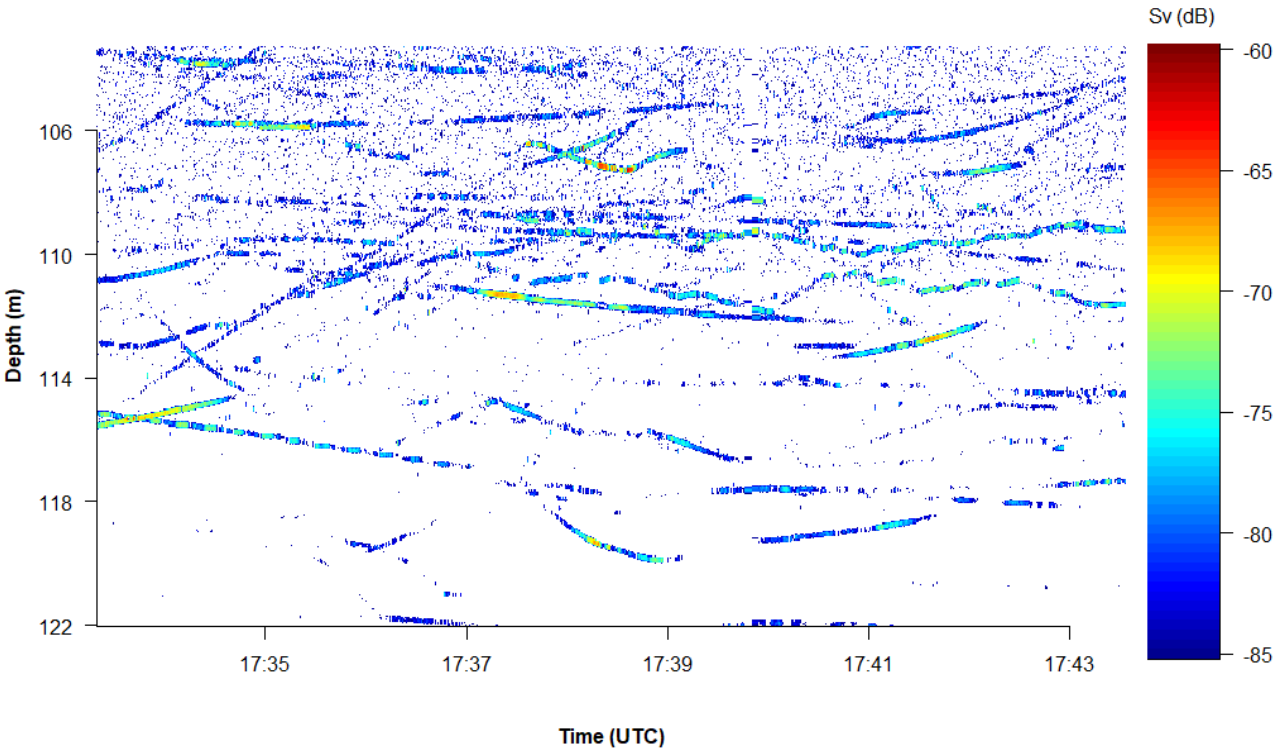

Fig. 19. Evening ekkogram right below the SSL. The layer had just started its dusk ascent. Record from 22.03.2020. Threshold: -85 dB.

3.3.2 August

Population Analysis

Also in August, we observed that the SSL carried out DVM behavior throughout the period, with little variation between days (Fig. 20A). However, the SSL spent shorter time in upper waters due to shorter summer nights. The general population would stay in near-surface waters for ~5 hours before descending again, inhabiting deeper waters throughout the longer summer days (Fig. 20A). Thus, the largest vertical range of the layer occurred early in the morning from ~45 m and down to the seabed (Fig. 20B). Noon distribution was at around 60 m and almost down to the seabed (Fig. 20C). It was also noticeable that there were two SSLs during nighttime. During the dusk ascent the population migrated up to a depth of about 10 m, and a second forming at ~30 - 60 m shortly after. We could not verify the exact depth distribution at night i.e., the uppermost depth the population would migrate to, due to high noise at long distances (Fig. 20B). We also observed that the deepest part daytime layer had strong S_v in the morning subsequent to the dawn descent, but gradually became faint as the

day progressed. Traces of strong scatterers moved into the upper part of the layer during the day (Fig. 20B).

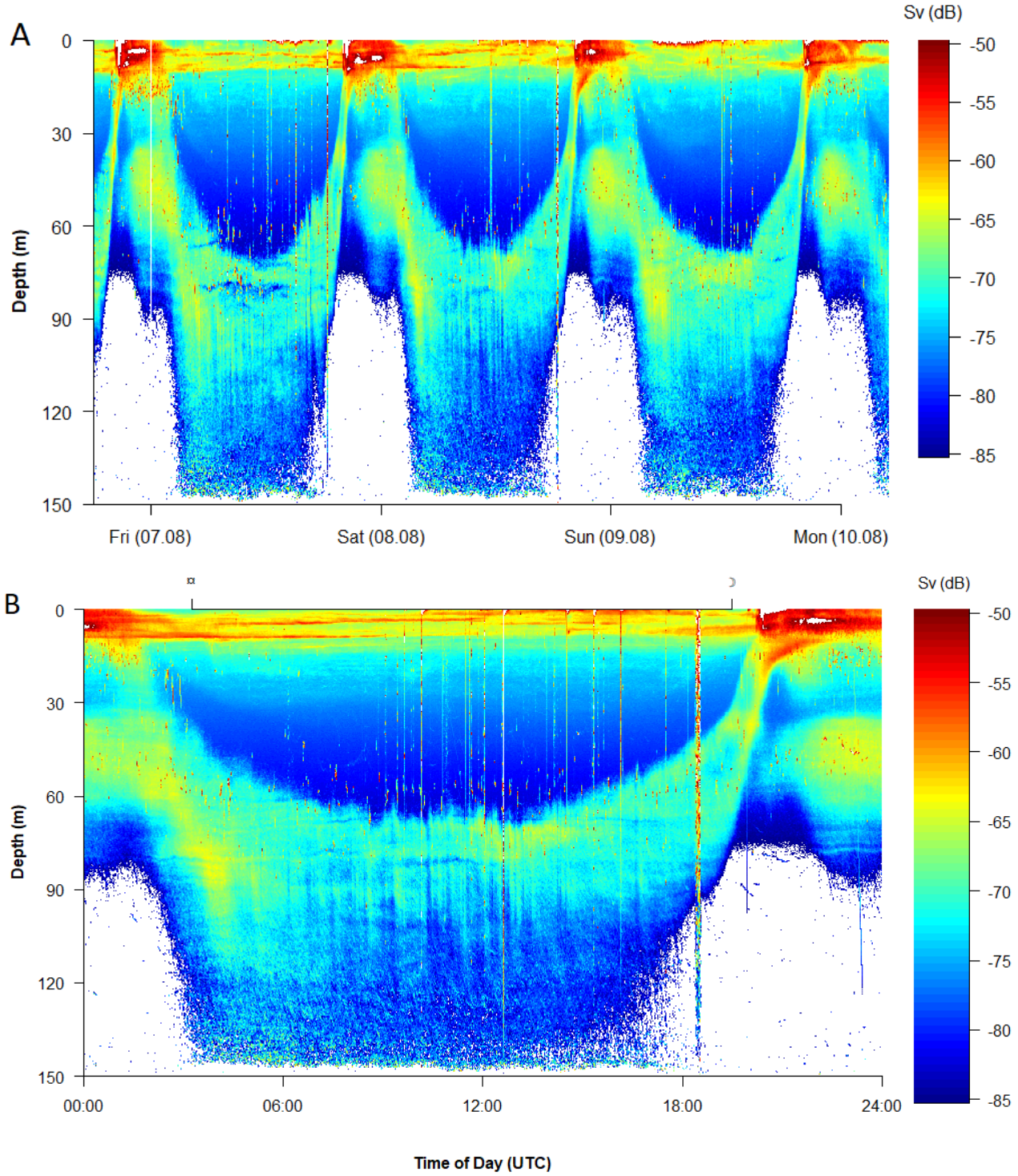

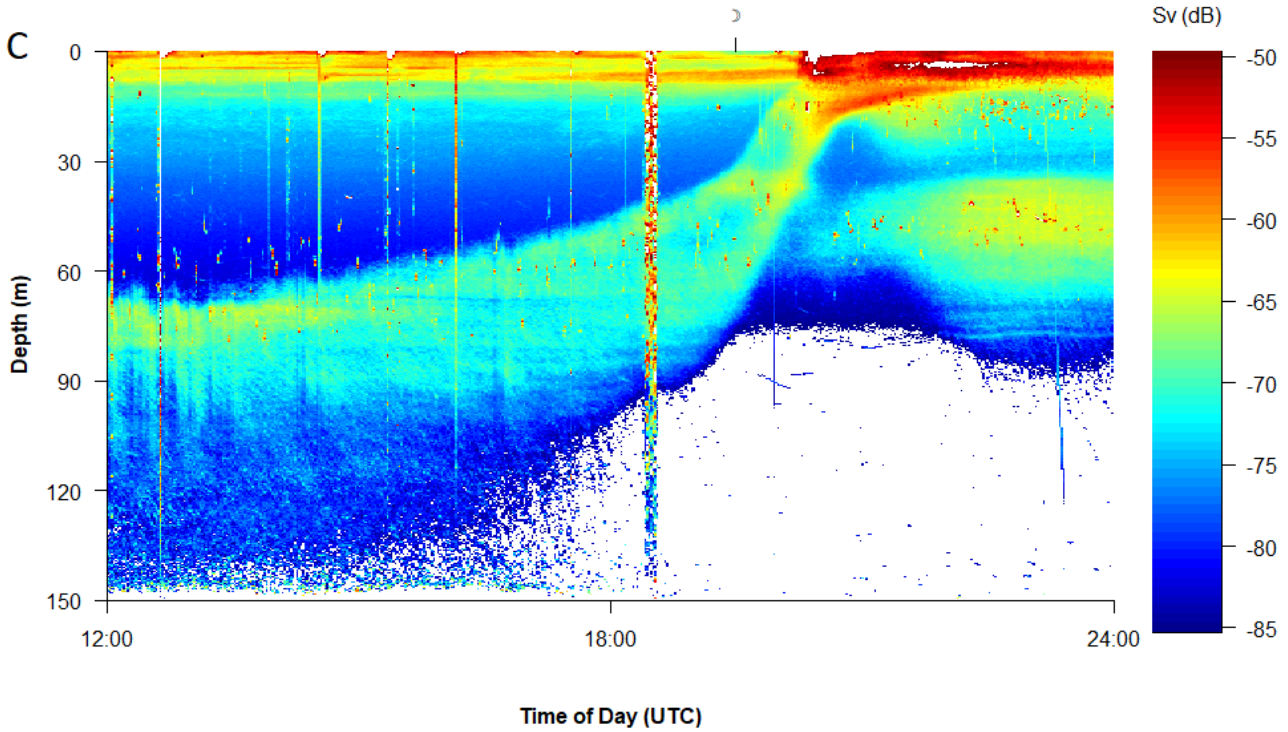

Fig. 20. August echogram data. A: August recordings summary (06.08.2020 – 10.08.2020). SSL has a longer duration in its daytime depth, and very short time periods in the shallows. B: Echogram from august field campaign displaying day- and night cycle of sound scattering layer. Daytime behavior was unlike that of March, threshold -85 to -50 dB. Daylength illustrated on top horizontal axis, sun (☼) symbol highlighting the time of sunrise, and crescent moon (☽) time of sunset. C: Afternoon to midnight recording (08.08.2020). Crescent moon (☽) at top axis marks the time of sunset.

Individual Behavior Analysis

Individual echo traces close to the transducer during the day displayed a general different type of behavior than in March, although some sinking traces were observed also in August (Fig. 21). Zooming in on the post-sunrise descent showed that traces were shorter and denser. Short traces meant that individual organisms did not stay in the echosounder's beam for long periods in deep waters but swam through it (more horizontal movement). In general, patterns were more straight-lined, going downwards and turning upwards. Due to weak traces of upwards moving individuals, we could not present 3D patterns of this type of behavior.

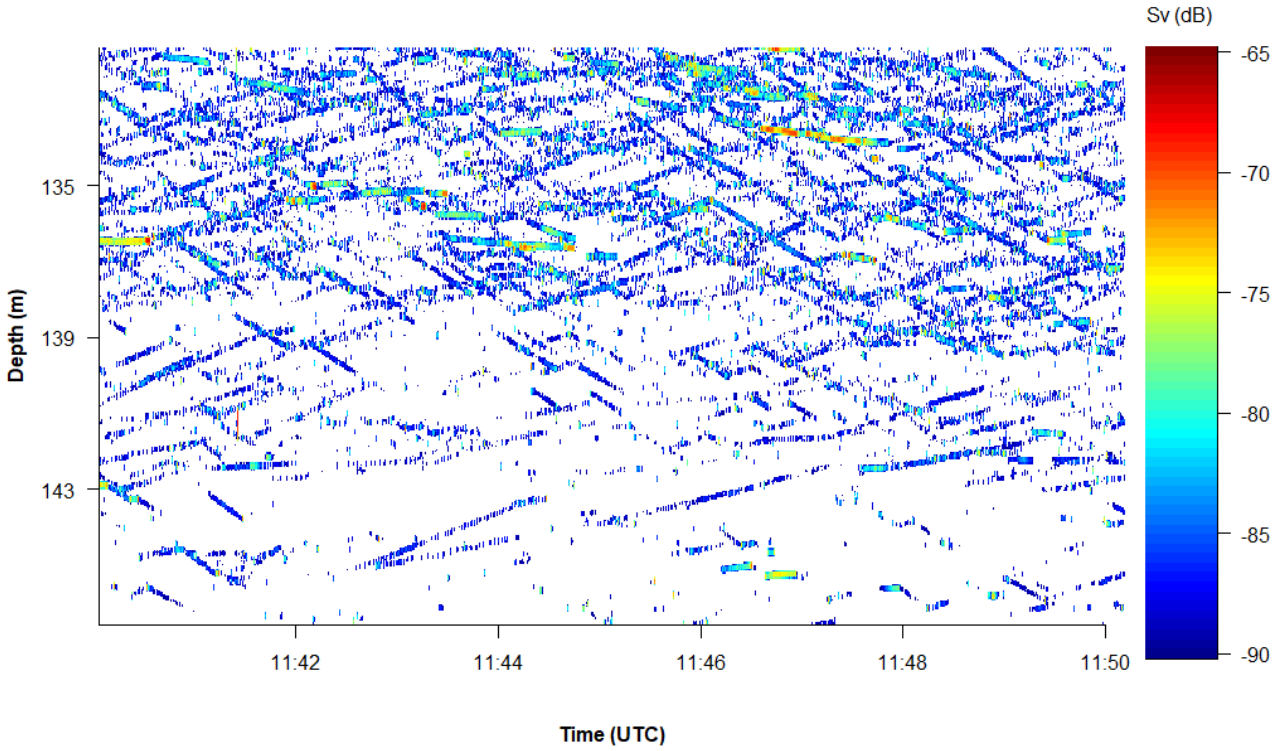

Fig. 21. Individual patterns of traces in August at noon (08.08.2020). Threshold: -90 dB, to visualize more upwards oriented movements.

3.3.3 October

Population Analysis

The entire population migrated (Fig. 22A), up at night, and down before day, the entire period. The krill layer migrated downwards between 05:00 and 07:00 UTC. Upwards migration occurred between 13:00 and 17:00. The migrations ended after the calculated sunrise and sunset times. Sunrise during the recording period was after 06:00 and sunset was a little before 16:00. Thus, the SSL had just completed its descent/ascent before the time of sunrise and sunset.

October acoustic data showed that the population had a much smaller vertical extension than earlier in the year. Daytime range of the layer was located at a range between 60 and 90 meters around noon (Fig. 22B), most densely aggregated upwards of 70 m. However, there was also a faint layer down to 110-120 m. The krill population did not descend closer to the transducer than 30 meters.

During the evening, the krill population migrated to a depth of about 10-15 m. This repeated itself in a uniform pattern throughout the entire period logged for the October data.

We also recorded repeated occurrences of voids in the daytime scattering layer. These were noticeable through the entire daytime between dusk descent and dawn ascent (Fig. 22B and C). We observed a layer of more intense backscatter above the krill layer at daytime, that was fish (Fig. 22).

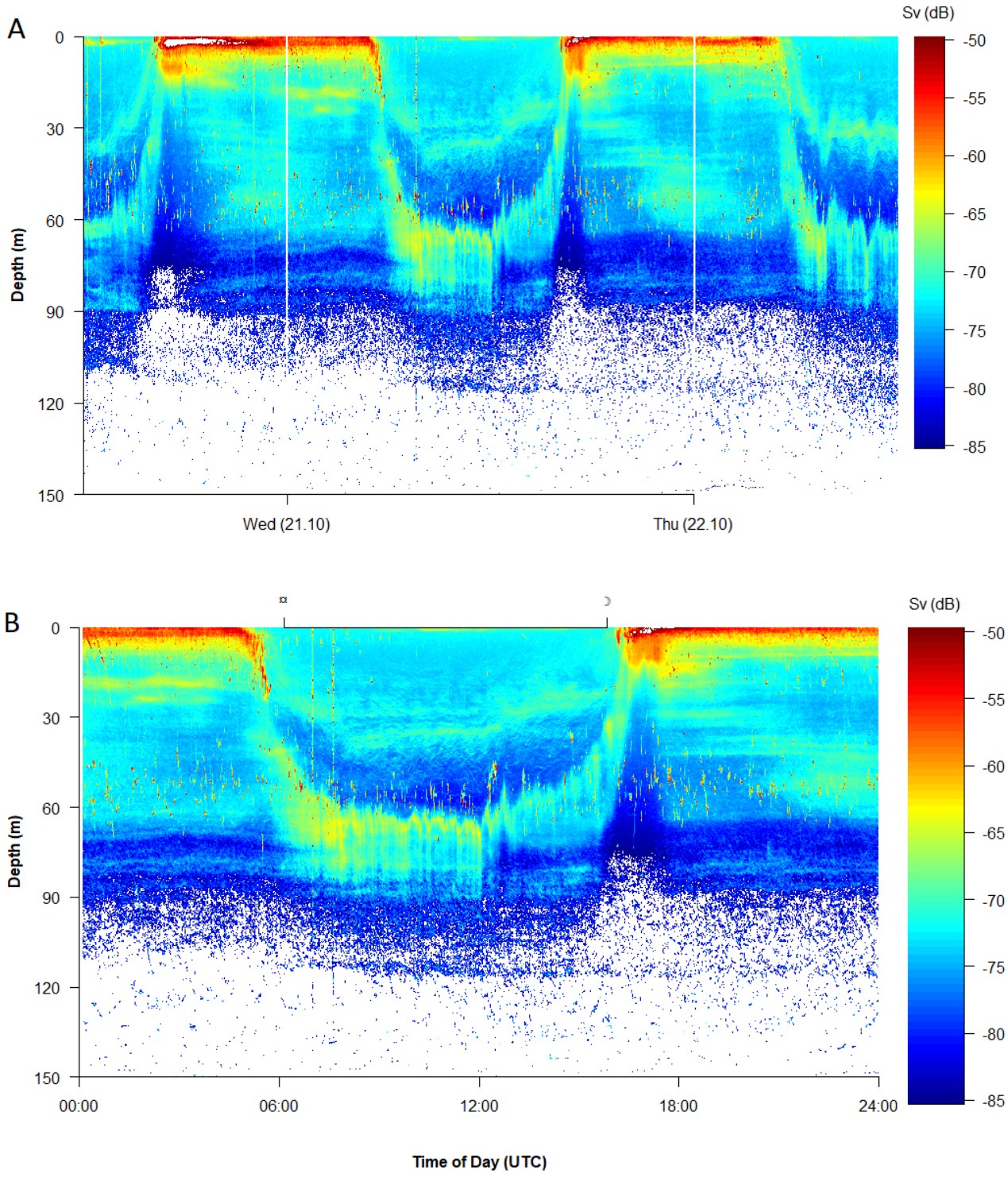
A
Sv (dB)
-50
-55
-60
-65
-70
-75
-80
-85
Depth (m)
0
30
60
90
120
150
Wed (21.10)
Thu (22.10)
B
Sv (dB)
-50
-55
-60
-65
-70
-75
-80
-85
Depth (m)
0
30
60
90
120
150
00:00
06:00
12:00
18:00
24:00
Time of Day (UTC)

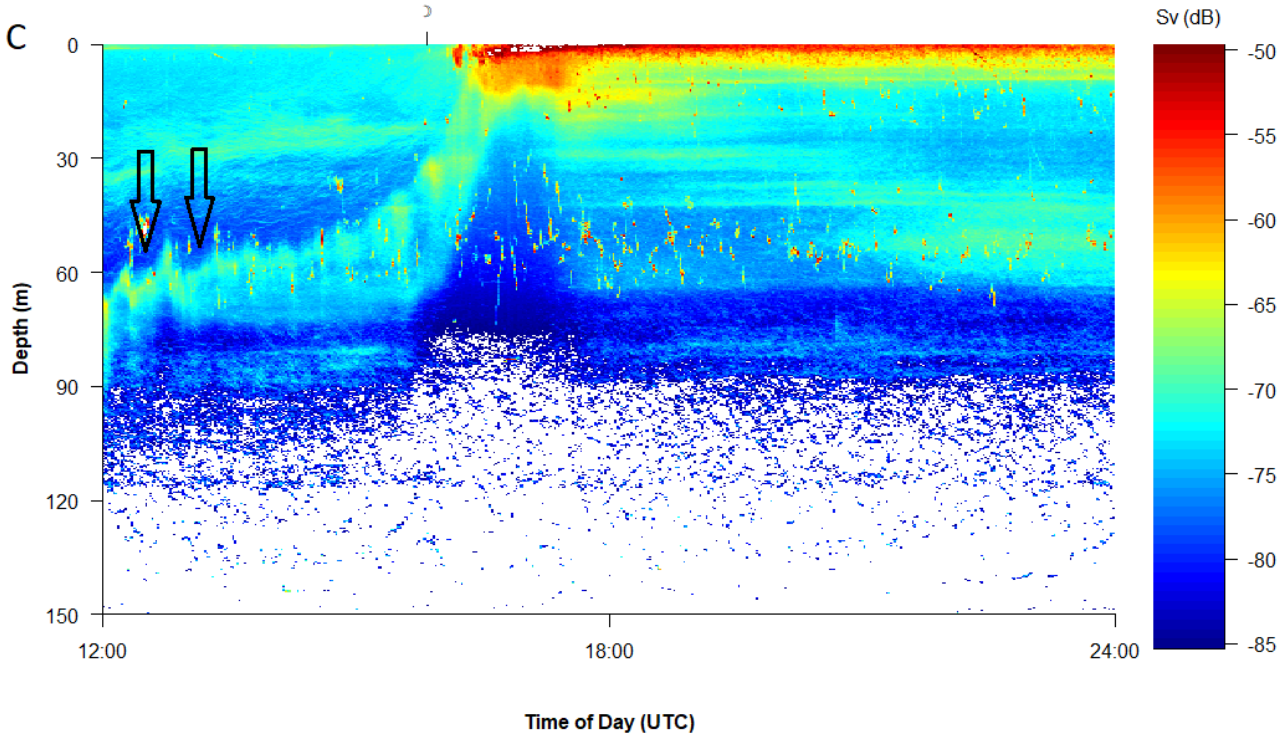

Fig. 22. October echogram data. A: Summary recordings from the October field recordings (20.10-20 – 22.10.20). Thresholds were -85 to -50 dB. Daytime krill layer displayed voids through the entire period as demonstrated here, and generally did not descend further than 110 – 120 m depth. B: 24-hour period starting and ending at midnight on 21.10.20. Top horizontal axis displays estimated times of sunrise (☼) and sunset (☽) on this date at the location (21.10.20). The population sank to deeper waters about 2 hours before sunrise and migrated upwards 1-2 hours before sunset. C: Half of a diel cycle period in October recordings (21.10.2020). Example to demonstrate the observable voids in the SSL, here in this case noticeable around 12:30, marked with arrows.

Individual Behavior Analysis

The lowest depths of the krill layer displayed similar behaviors to that of August, although higher up in the water column. The long echo traces shown in Fig. 23 was because of the spread of the echo beam with increasing range. Continuous traces show that they remained level by constantly going upwards and downwards again, here avoiding crossing ~120 m. Hence, the zigzag pattern observed above the mostly blank space that is depths with no acoustic backscatter (Fig. 23). 3D patterns in October were not conducted due to weaker traces and long range.

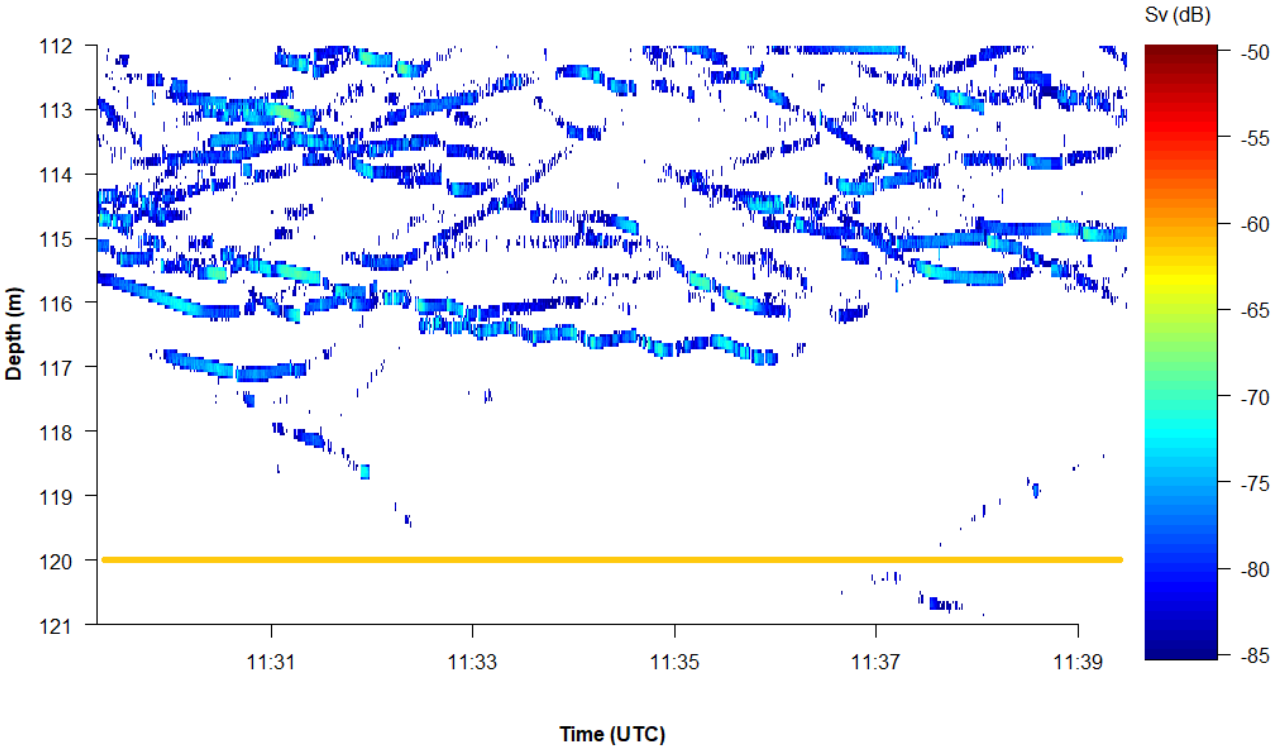

Fig. 23. Close-up example at noon from ~110-120 m depth). The yellow line illustrates a deep limit where individual krill traces generally did not move past.

3.3.4 Fish data

We presented the fish data by using a higher threshold which removes krill echoes (lower threshold of -65 dB).

Fish was in general only present in the upper parts of the krill layer at daytime. In March, fish echoes were vertically spread out during the day (Fig. 23A), from ~30 to ~100 m. Nighttime traces were between ~30 and ~60 m. Fish traces followed the krill layer during ascent and descent, and were inside the krill layer (see also Fig. 16A - C), where they formed dense aggregations. There were schools of fish above the krill layer at ~30 m, that followed the dusk ascent, but remained above the krill layer (see also Fig. 16A - C) From our data we could demonstrate that fish in the study area expand their vertical distribution with ~30 m from nighttime to daytime.

In August, longer daylength caused fish traces to aggregate for shorter periods during night but followed the dawn descent deeper. They moved also to a deeper range during the day, ~60 to ~90 m (Fig. 24B). Deeper range of fish would sometimes cause voids at the top of the krill layer when encountered (Fig. 25A). Strong echoes in near-bottom waters in March and August are gas bubbles released from the echosounder rig.

In October, the fish distribution was narrower during daytime, from ~45 to ~70 m (Fig. 24C). Voids on top of the daytime krill layer became much more frequent as fish traces and the krill layer were in closer proximity (Fig. 25B, see also Fig. 22C). Fish did not appear to reside inside the SSL, or following it during migrations.

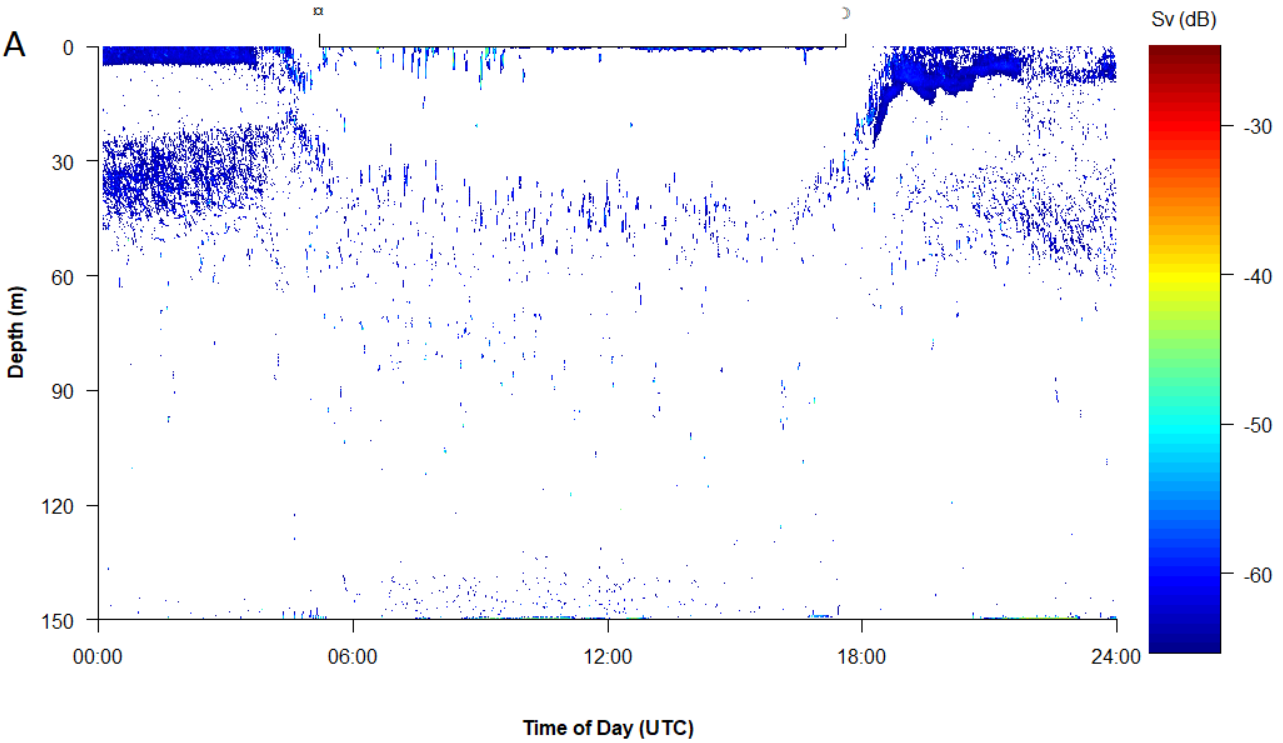
A
Sv (dB)
-30
-40
-50
-60
Depth (m)
0
30
60
90
120
150
00:00
06:00
12:00
18:00
24:00
Time of Day (UTC)

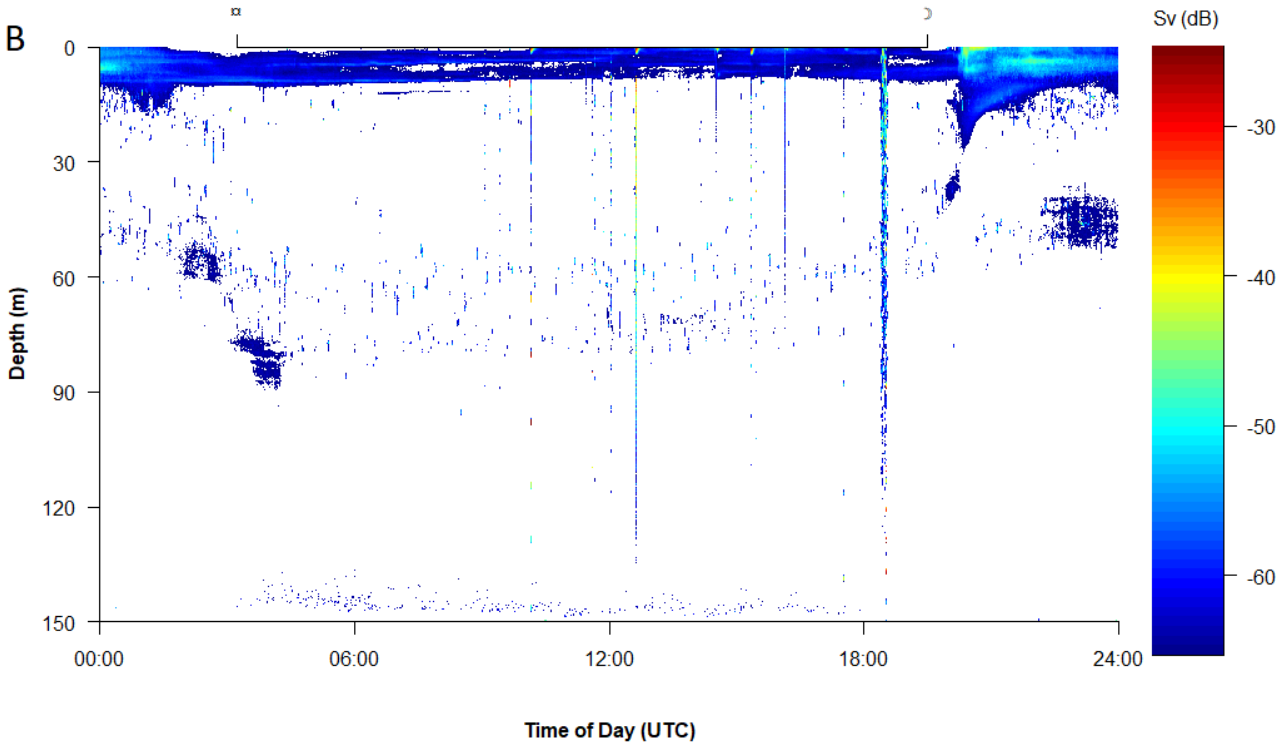
B
Sv (dB)
-30
-40
-50
-60
Depth (m)
0
30
60
90
120
150
00:00
06:00
12:00
18:00
24:00
Time of Day (UTC)

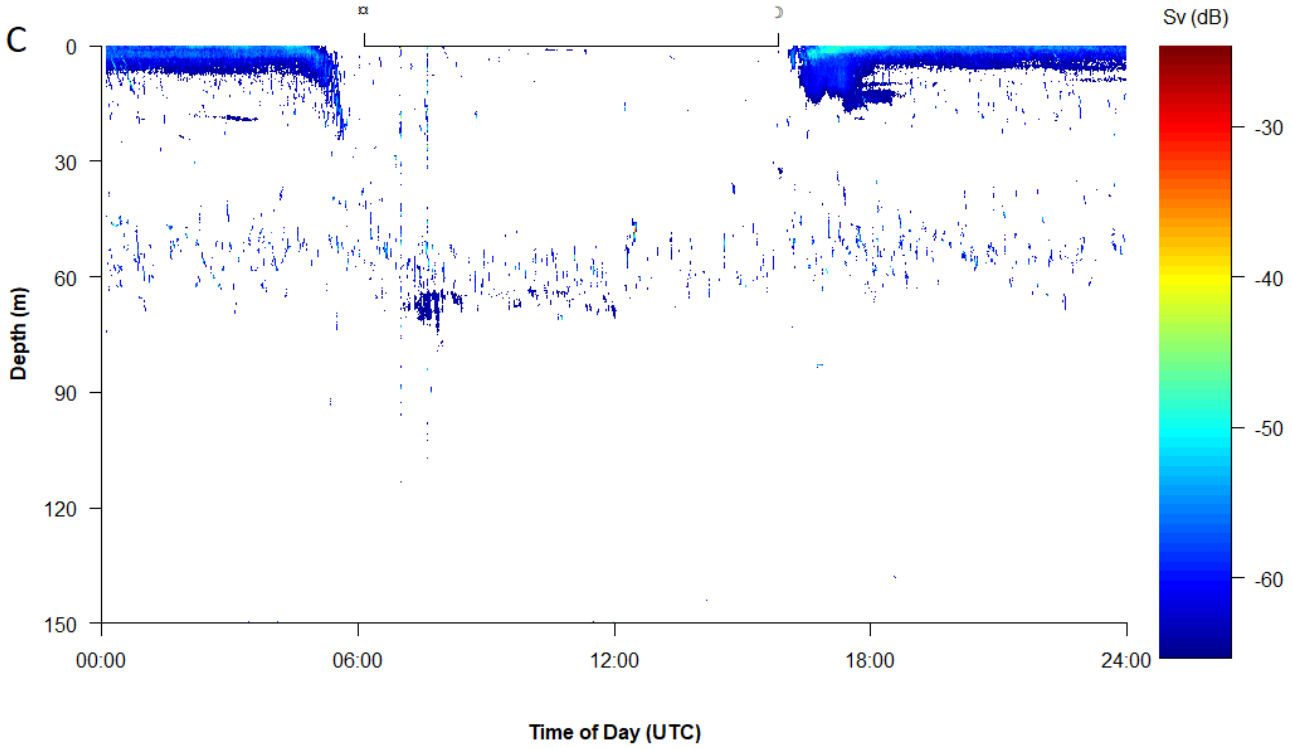

Fig. 24. Fish acoustics in all seasons. Adjusted threshold for 22.03.2020, 08.08.2020 and 21.10.2020 (same days as selected days of krill analyses). A: Spring, B: Summer, C: Autumn. Sun and moon symbols on top horizontal axis gives times of sunrise (☼) and sunset (☽).

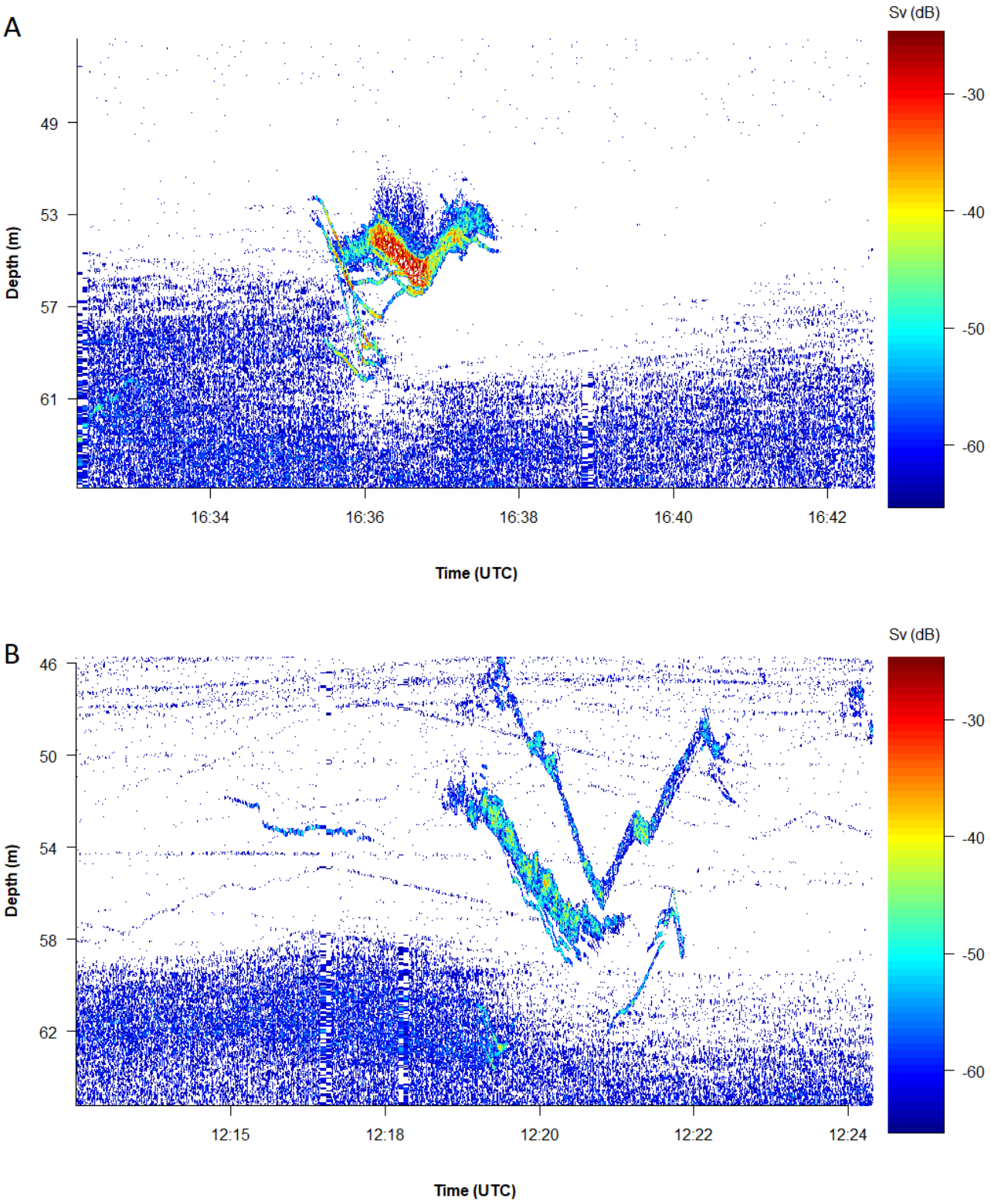

Fig. 25. Examples of voids in upper part of krill SSL caused by diving fish. A: August afternoon recording (07.08.2020). B: October recorded fish dive to the top of the krill layer at noon (21.10.2020). Pictures collected from RStudio, by exporting sample data from Sonar5-Pro.

4 Discussion

Across all recorded seasons, the krill population carried out DVM behavior, but with some differences in pattern. Also, our findings demonstrate that both on a population level and on an individual level, the krill displayed a variety of behaviors across the seasons. Although swimming behavior at depth were different, krill were also observed at the same depths in August. In October, krill were not observed in near-bottom waters. Most of the population had a maximum depth border that they did not cross (120 m), even though a few individuals were observed swimming below it.

Fish were observed mostly above or at the top of the krill layer. Here, we repeatedly observed krill displaying escape reactions. Deeper living krill were not particularly exposed to predation. From this, we interpret that their daytime behaviors were likely related to other factors, such as feeding.

4.1 Spring

Spring recordings showed that the population's DVM pattern involved coming all the way down to the bottom, displaying a long vertical range, with individual analysis revealing continuous sinking in a conspicuous pattern, in the deepest waters.

Krill were observed sinking the entire way down to the seafloor, despite a recorded oxygen concentration of <2 mg/l (Fig. 17, Fig. 8). We also observed an increase in fluorescence depth. This suggests that there was potentially substantial food supply at these depths, that sinking krill could correlate with. Phytoplankton is an important food source in the diet of *M. norvegica* (Schmidt, 2010). Indeed, laboratory experiments has shown that *M. norvegica* (in comparison with another krill species, *Thysanoessa raschii*) display a type III (sigmoidal curve) response to increasing concentrations of phytoplankton, indicating that there could be a threshold concentration that must be exceeded for krill to efficiently forage on these (Cabrol et al., 2020; Holling, 1959). It may be that this 'threshold' is exceeded in deeper waters in late spring after the bloom and is the reason for our acoustic observations during the day. Without having biological samples from this campaign, we could not verify that krill fed on algae in late March. However, krill stomach fluorescence have been found on late afternoons around the time of the spring bloom termination previously (Kaartvedt et al., 2002; Onsrud &

Kaartvedt, 1998). Because of this we suggest that *M. norvegica* must have grazed on phytoplankton in our study as well.

Significant portions of the vertical transport of carbon stems from phytoplankton blooms (Turner, 2002), suggesting foraging at depths subsequent of blooms. In March, sinking in circles was a prevailing behavior. It may be that the sinking pattern displayed at these depths is a method for filtering phytoplankton.

There were also some sinking patterns during the evening ascent. If related to feeding, sinking behavior may be related to feeding on a deep food source while migrating. It could be that already satiated krill don't complete their migration to upper waters and sink immediately to digest, as discussed in Kaartvedt (2010). However, the whole population appeared to ascend to upper waters. Krebs & Davies (1978) stated that an animal should maximize their energy gain from foraging, and that time spent searching for and handling resources should not exceed the energy gain from resource intake. We argue that the migration upwards before sunset contributes to a krill's search time. Yet, there may be a greater reward by completing the ascent to upper waters. The fluorescence profile showed that most of the fluorescence was in the shallows, and that this is a richer feeding ground. Indeed, increased stomach fluorescence during nighttime in March has been reported in Klevjer & Kaartvedt (2011). If *M. norvegica* didn't complete a dusk ascent entirely, they could reduce predation risk and energy expenditure but gain less.

Since phytoplankton also is grazed on and digested in deeper waters such as in the population's daytime depth distribution, this could have implications for our understanding of the carbon pump. Specifically the speed of carbon transport, since krill pellets play a role in this mechanism (Turner, 2002). We suspect that krill can add to this effect by grazing at large depths in their deep daytime habitat in addition to their upper water feeding at night. Røstad & Kaartvedt (2013) demonstrated that the sedimentation rates increases with pellet size, and found that fecal pellets were most present in the deep at daytime in late spring. Also, it has been observed that sinking speeds of krill fecal pellets may largely be affected by their phytoplankton diet components. For example, the Antarctic krill (*Euphausia superba*) can produce faster sinking pellets when feeding on diatoms (Cadée et al., 1993). Species composition of deep sinking algae subsequent a bloom in the Bunnefjord could give more insight to how much an effect daytime grazing could be in spring. The possible effect on the

speed of this mechanism could be of interest for example in mapping effects of DVM on carbon transports in the oceans (Archibald et al., 2019; Honjo et al., 2008).

The constant individual sinking during the daytime distribution of the population but no aggregation into an additional layer closer to the seabed suggests that krill swim back up at some point. Acoustic target strength is strongly related to tilt angle (Klevjer & Kaartvedt, 2006). Vestheim et al. (2014) demonstrated that krill in an upwards swim is not visible on 120 kHz resolution. However, ascending individuals were observed with 200 kHz, even. Closer to the transducer we could document some upwards swimming, although faint.

We conclude that krill swim back up after sinking and must do this several times during the day. From our findings from average sinking speeds (6.84 $mm \cdot s^{-1}$), it would take an individual krill about 3 h 15 min to sink through the daytime layer and down to the bottom, assuming the sinking occurs from the layer and no variations in time of day (Table 2). The daytime distribution lasted for ~12 h 30 min (05:00 – 17:30). We assume that deep sinking individual krill was not motivated by or followed other external cues during the day, and maintained a constant upward swim (Hardy & Bainbridge, 1954). Our observations in March suggested an upwards swim of 21 $mm \cdot s^{-1}$ which adds to then ~76 $m \cdot h^{-1}$. This would result in almost three trips, but at least two before the onset of the dusk ascent. Our suggested swimming speeds roughly coincides with daytime speeds found in De Robertis et al. (2003), although in a different species and season. Sourisseau et al. (2008) suggested a vertical migration speed for *M. norvegica* of 42 $mm \cdot s^{-1}$, and argued that this was roughly in consensus with experimental results from Hardy and Bainbridge (1954) and Thomasson et al. (2003), and acoustic observations in Tarling et al. (1999). This is faster than our suggested upwards swimming speed in March. If this is the case, individual *M. norvegica* could conduct even more trips from the seafloor up to the SSL. It must be noted however, that other suggested swimming speeds were mainly associated with DVM behavior, not individual behavior during daytime in deep waters.

Such repeated vertical swimming has implications for our understanding of krill energy budgets. Torres & Childress (1983) explained through laboratory experiments on oxygen consumption and temperature that krill DVM is energetically costly and that it outweighs any reward from residing in deeper colder waters by day. However, we have observed that not only do krill swim when they migrate upwards at night, they also do repeated migrations up and down within the population's daytime distribution and the seabed throughout the day. By

migrating 80 m to the top of their daytime layer several times during daytime would mean that the daytime vertical swimming exceeds the distance of swimming to upper waters during the dusk ascent (~70 – 140 m) in a day. Because of such vertical relocations of individuals, we expect the size distributions in March not to show any trend by depth. Lacking field samples, however, we could not confirm this.

Jaffe et al. (1999) argued that through reduced swimming activity, individual krill save energetic cost. Extending sinking periods through circling may be advantageous. This type of behavior was less common in the following seasons.

By sinking down through the SSL and down to 150 m depth the krill sink through several orders of magnitude in light levels. Vestheim et al. (2014) suggested one order of magnitude per ~15 m depth, in the Bunnefjord. Since we found them to sink the entire way to the seafloor, we assume they sank from 70 to 150 m depth. By sinking 80 m for every tour taken back up to the top of the daytime layer, an individual experiences a fluctuation of ~5 orders of magnitude less incoming light. While the upper portion of the krill layer follows an isolume in the afternoon (Hobbs et al., 2021; Onsrud & Kaartvedt, 1998), individual krill do not follow isolumes during daytime.

4.2 Summer

As the seasons progressed, we observed a different pattern in DVM, and individual behavior in deeper waters in August.

The field samples yielded catches of krill in all sample depths throughout the krill layer with catch size increasing with depth and fits with our acoustic observation of the SSL that came the entire way down to the seabed. We registered low levels of oxygen in the deep (<2 mg/l, 21% saturation). Even though, *M. norvegica* has low tolerance for poor oxygen conditions (Spicer & Saborowski, 2010), they can for limited time enter hypoxic waters (Spicer et al., 1999).

Size distributions showed smaller krill with increased depth. This is a contrast to what usually have been the case in the Oslofjord historically, with krill size increasing with depth (Klevjer & Kaartvedt, 2006). Our records showed a strong scattering layer coming down to the seabed after the dawn descent and became fainter as the day progressed. If swimming capacity

increases with size (Thomasson et al., 2003), it may be that larger krill had swum to the upper parts of the daytime layer's range by noon while smaller krill were gradually remaining behind when we conducted our sampling. Furthermore, with tilt angle of up- or downwards swimming krill explaining the deeper part of the layer having a weaker backscatter and gradually becoming more faint (Klevjer & Kaartvedt, 2006). Without tow samples from other parts of the daytime, we could not test this. Elsewhere it has been shown in *Euphausia superba* that larger krill remain deeper during daytime when large diving predators are nearby (Ichii et al., 2020). Yet in our recordings, larger krill came up to the upper parts of the SSL while possible predators were patrolling these waters.

We recorded a different type of behavior in the deep waters at daytime compared to spring. Individual krill traces in deep waters from this period suggested shorter time spent in the acoustic beam. Individual vertical swimming paths of *Euphausia pacifica* was found generally to be more diagonal than directly upwards or downwards (De Robertis et al., 2003), which could explain shorter traces observed at depth. From this we argue that they swim more actively at least in deep waters at day. As demonstrated by Kaartvedt et al. (2002), krill can switch diets from spring to late summer, as they have been found to have more calanoid mandibles in their guts at this time relative to the spring situation when they had high gut fluorescence. Abrahamsen et al. (2010), found that *M. norvegica* conducted a majority of attacks on prey located below their ventral side as opposed to above their dorsal side. This may be the reason for the subsequent upwards and downwards swimming pattern we have observed in summer recordings. Krill may be diving down to attack their prey, and subsequently reset by swimming back upwards again. Indeed, gut mandibles were most abundant in the deepest krill samples. From these findings it is reasonable to assume that deep swimming *M. norvegica* in the Bunnefjord are foragers that display a behavioral shift from spring to summer. Kaartvedt et al. (2002) argued that *M. norvegica* has a higher gain in terms of carbon uptake from feeding on animal food sources, and that these should be the preferred diet when abundant (Krebs & Davies, 1978). This is reasonable because copepods can accumulate large amounts of lipids (Kattner & Hagen, 2009; Lee & Hirota, 1973), and are energetically beneficial as prey items. Cabrol et al. (2020) has also shown that *M. norvegica* display a type III functional response to increasing densities of zooplankton, with phytoplankton present. It may be that the changes we have observed in general individual behavior are related to their foraging habits when krill effectively switch diet to zooplankton, such as copepods. We should note that according to Gerritsen and Strickler (1977) increased

speed increase encounter with prey. Unfortunately, we could not confirm from our study that krill had a more carnivorous diet in summer compared to spring. However, stomach analyses did yield calanoid mandibles in summer samples, hence we could confirm that krill indeed did forage on copepods at this time.

4.3 Autumn

In October krill conducted DVM but did not migrate down to similar depths as previously recorded. Individual krill displayed similar patterns as in summer, but higher up in the water column following oxygen constraints in the deep.

Fig. 13 demonstrated that the largest catch sizes from IKMT sampling occurred at 70 m and 90 m depths, which conformed with our acoustic data (Fig. 22). Our catches verified that this indeed was krill that formed the layer, and fits with previous studies in the Bunnefjord (Klevjer & Kaartvedt, 2011; Solberg et al., 2012; Vestheim et al., 2014). In October, both catches and acoustic records had a narrower vertical distribution range than the former study periods as the population tended to avoid the deepest parts. The denser SSL avoided waters below ~90, but a faint layer had a range down to even ~120 m. Bottom depths were avoided altogether. This may be a result of the poorer oxygen conditions as the seasons progressed and the lower range of the main krill layer occurred at depths with dissolved oxygen concentrations of 0.9 mg/l, with the faint layer coming down to depths with concentrations of ~0.67 mg/l.

These findings fit with expectations of low oxygen levels towards the seabed, followed by deep waters devoid of backscatter in late autumn in Bunnefjord (Solberg et al., 2015).

However, we did observe a few individuals surprisingly swimming below 120 m where oxygen concentration was <0.67 mg/l. This was an interesting find due to growing concerns over deoxygenation in the world's oceans, and what this could mean for zooplankton (Breitburg et al., 2018; Levin, 2018; Stramma et al., 2010; Tremblay et al., 2020; Wishner et al., 2018). Based on our data, we suggest that *M. norvegica* has a general lower tolerance level of ~0.67 mg/l (~7.02% saturation). This was the measured O_2 around the "invisible bottom" at 120 m that the krill population generally did not cross during daytime. Hypoxia tolerances in krill has been linked with their DVM behavior, and that special adaptations must be in place for an organism to migrate across places of fluctuating environmental parameters

(Tremblay et al., 2020). Tremblay et al. (2020) showed that different species have adapted different strategies to cope with oxygen constraints in some of the world's upwelling areas, and that some species of krill lower their respiration rate with decreasing temperature and oxygen saturation. It has been observed that at least one species of krill can even tolerate periods in anoxic waters during their daytime DVM activities (Riquelme-Bugueño et al., 2020). Although *M. norvegica* may not survive anoxia, they have been shown to still carry out DVM behaviors despite oxygen constraints (Spicer et al., 1999), but this is dependent on the temperature of the deep they descend to (Strömberg & Spicer, 2000). It may be that krill in the Bunnefjord are able to cope with low oxygen levels during the day in deeper waters if their oxygen expenditure is lowered enough if an adequate low temperature - low oxygen combination is met. Following results from Saborowski et al. (2000), we could even argue that residing intermittently in the colder deep provides relief from the increased oxygen demand associated with staying in warmer waters. Lastly, Klevjer & Kaartvedt (2011) argued that *M. norvegica* regulated their oxygen needs though reduced swimming. This may be the reason for vertically narrow zigzag patterned echo traces, as krill merely move up and sink to stay level at their lowest tolerance depth. While doing so, they could also reduce predator encounter (Gerritsen & Strickler, 1977).

Our records demonstrate that the krill population in Bunnefjord must cope with limited available vertical space when the low oxygen in the deeper waters prevent them from staying in deeper waters during the day. Fish were a possible predation threat and caused repeated voids on top of the layer. During a day in late October, it seems as if the krill population in the Bunnefjord was pressed in between unfavorable conditions in the deep and the upper daytime isolume, followed by fish in the shallows. Our data show that fish were interacting with krill in October. However, fish going into the layer at day was not as prominent. It was unclear if krill in the Bunnefjord was heavily predated in this period.

Poor oxygen conditions force deep-living organisms up from expanding Oxygen Minimum Zones (OMZ), which might increase their predation risk (Koslow et al., 2011; Netburn & Koslow, 2015). However, it is not clear if this would increase predation risk of krill in our study. While the krill population may have been forced upwards to a shallower depth, fish were also displaced upwards.

5 Conclusion

The deployment of an autonomous submerged echosounder enabled studying the krill population in the Bunnefjord. It also enabled studying individual krill. The results show that this method is an effective way of observing behavioral biology *in situ.* Biologically the population always conducted DVM, with some variations depending on seasonal daylength. Deep-living individuals had two prominent behaviors that differed from between spring to summer and autumn in during daytime, and we suggest that these were related to foraging.

Future studies may involve expansions to other regions and periods to see if the behavioral patterns observed here are recurring behaviors or if they are specific for geographic reasons or seasons rather than short-term fluctuations. Also, more extensive stomach analyses might help interpreting particular swimming patterns.

Studies of krill behavior in different environmental conditions, may reveal other forms of swimming behavior in deep waters. More studies may provide more precise information about oxygen tolerance levels in krill, and how well *M. norvegica* specifically will cope with a potentially more deoxygenated ocean.

References

Abrahamsen, M. B., Browman, H. I., Fields, D. M., & Skiftesvik, A. B. (2010). The three-dimensional prey field of the northern krill, *Meganyctiphanes norvegica*, and the escape responses of their copepod prey. *Marine Biology*, *157*(6), 1251–1258. https://doi.org/10.1007/s00227-010-1405-9

Archibald, K. M., Siegel, D. A., & Doney, S. C. (2019). Modeling the impact of zooplankton diel vertical migration on the carbon export flux of the biological pump. *Global Biogeochemical Cycles*, *33*(2), 181–199. https://doi.org/10.1029/2018GB005983

Balk. (2021). *Balk et al. 2021. Sonar4 and Sonar5-Pro post processing systems, Operator manual version 606.22, 489p. Cage Eye A/S. Enterprise: NO 970142 959 MVA / VAT* (606.22) [Computer software]. NO 970142 959 MVA / VAT.

Barange, M., Gibbons, M. J., & Carola, M. (1991). Diet and feeding of *Euphausia hanseni* and *Nematoscelis megalops* (Euphausiacea) in the northern Benguela Current: Ecological significance of vertical space partitioning. *Marine Ecology Progress Series*, *73*(2/3), 173–181. JSTOR.

Berge, J., Cottier, F., Varpe, Ø., Renaud, P. E., Falk-Petersen, S., Kwasniewski, S., Griffiths, C., Søreide, J. E., Johnsen, G., Aubert, A., Bjærke, O., Hovinen, J., Jung-Madsen, S., Tveit, M., & Majaneva, S. (2014). Arctic complexity: A case study on diel vertical migration of zooplankton. *Journal of Plankton Research*, *36*(5), 1279–1297. https://doi.org/10.1093/plankt/fbu059

Beyer, F. (1968). Zooplankton, zoobenthos, and bottom sediments as related to pollution and water exchange in the Oslofjord. *Helgoländer Wissenschaftliche Meeresuntersuchungen*, *17*(1–4), 496–509.

Breitburg, D., Levin, L. A., Oschlies, A., Grégoire, M., Chavez, F. P., Conley, D. J., Garçon, V., Gilbert, D., Gutiérrez, D., Isensee, K., Jacinto, G. S., Limburg, K. E., Montes, I.,

Naqvi, S. W. A., Pitcher, G. C., Rabalais, N. N., Roman, M. R., Rose, K. A., Seibel, B. A., … Zhang, J. (2018). Declining oxygen in the global ocean and coastal waters. *Science*, *359*(6371), eaam7240. https://doi.org/10.1126/science.aam7240

Brusca, R. C., Moore, W., Shuster, S. M., & Brusca, G. J. (2016). *Invertebrates* (3rd Edition). Sinauer Associates.

Cabrol, J., Fabre, A., Nozais, C., Tremblay, R., Starr, M., Plourde, S., & Winkler, G. (2020). Functional feeding response of Nordic and Arctic krill on natural phytoplankton and zooplankton. *Journal of Plankton Research*, *42*(2), 239–252. https://doi.org/10.1093/plankt/fbaa012

Cadée, G. C., González, H., & Schnack-Schiel, S. B. (1993). Krill diet affects faecal string settling. In G. Hempel (Ed.), *Weddell Sea Ecology* (pp. 75–80). Springer. https://doi.org/10.1007/978-3-642-77595-6_8

Christiansen, S., Titelman, J., & Kaartvedt, S. (2019). Nighttime swimming behavior of a mesopelagic fish. *Frontiers in Marine Science*, *6*. https://doi.org/10.3389/fmars.2019.00787

Dalpadado, P., & Skjoldal, H. R. (1991). Distribution and life history of krill from the Barents Sea. *Polar Research*, *10*(2), 443–460. https://doi.org/10.1111/j.1751-8369.1991.tb00665.x

De Robertis, A., Schell, C., & Jaffe, J. S. (2003). Acoustic observations of the swimming behavior of the euphausiid *Euphausia pacifica* Hansen. *ICES Journal of Marine Science*, *60*(4), 885–898. https://doi.org/10.1016/S1054-3139(03)00070-5

Denny, M. (2008). *How the Ocean Works: An Introduction to Oceanography*. Princeton University Press.

Erazo, N. (2018, January 29). Tutorial: How to make a map using QGIS. *The Bowman Lab*. https://www.polarmicrobes.org/tutorial-on-qgis-how-to-make-a-map/

Foote, K. G. (1987). Calibration of acoustic instruments for fish density estimation: A practical guide. Int. Coun. Explor. *Sea Coop. Res. Rep.*, *144*, 1–69.

Frigstad, H., Harvey, T., Deininger, A., & Poste, A. (2020). *Increased light attenuation in Norwegian coastal waters—A literature review* (NIVA-Report M–1808; 7551-2020). Norwegian Institute for Water Research (NIVA). https://www.miljodirektoratet.no/publikasjoner/2020/november-2020/increased-light-attenuation-in-norwegian-coastal-waters/

Gerritsen, J., & Strickler, J. R. (1977). Encounter Probabilities and Community Structure in Zooplankton: A Mathematical Model. *Journal of the Fisheries Research Board of Canada*, *34*, 73–82. https://doi.org/10.1139/f77-008

Gibbons, M. J., Barange, M., & Pillar, S. C. (1991). Vertical migration and feeding of *Euphausia lucens* (Euphausiacea) in the Southern Benguela. *Journal of Plankton Research*, *13*(3), 473–486. https://doi.org/10.1093/plankt/13.3.473

Gibbons, M. J., Pillar, S. C., & Stuart, V. (1991). Selective carnivory by *Euphausia lucens*. *Continental Shelf Research*, *11*(7), 625–640. https://doi.org/10.1016/0278-4343(91)90016-Y

Hardy, A. C., & Bainbridge, R. (1954). Experimental observations on the vertical migrations of plankton animals. *Journal of the Marine Biological Association of the United Kingdom*, *33*(2), 409–448. Cambridge Core. https://doi.org/10.1017/S0025315400008456

Hassel, A., Endresen, B., Martinussen, M., Knutsen, T., & Johannessen, M. E. (2013). Håndbok for prøvetaking og pre-analyse av plankton. *133 s.* https://imr.brage.unit.no/imr-xmlui/handle/11250/191650

Hays, G. C. (2003). A review of the adaptive significance and ecosystem consequences of zooplankton diel vertical migrations. In M. B. Jones, A. Ingólfsson, E. Ólafsson, G. V.

Helgason, K. Gunnarsson, & J. Svavarsson (Eds.), *Migrations and Dispersal of Marine Organisms* (pp. 163–170). Springer Netherlands. https://doi.org/10.1007/978-94-017-2276-6_18

Hobbs, L., Banas, N. S., Cohen, J. H., Cottier, F. R., Berge, J., & Varpe, Ø. (2021). A marine zooplankton community vertically structured by light across diel to interannual timescales. *Biology Letters*, *17*(2), 20200810. https://doi.org/10.1098/rsbl.2020.0810

Holling, C. S. (1959). The components of predation as revealed by a study of small-mammal predation of the European pine sawfly. *The Canadian Entomologist*, *91*(5), 293–320. https://doi.org/10.4039/Ent91293-5

Holtedahl, H. (1967). Notes on the formation of fjords and fjord-valleys. *Geografiska Annaler: Series A, Physical Geography*, *49*(2–4), 188–203. https://doi.org/10.1080/04353676.1967.11879749

Honjo, S., Manganini, S. J., Krishfield, R. A., & Francois, R. (2008). Particulate organic carbon fluxes to the ocean interior and factors controlling the biological pump: A synthesis of global sediment trap programs since 1983. *Progress in Oceanography*, *76*(3), 217–285. https://doi.org/10.1016/j.pocean.2007.11.003

Ichii, T., Mori, Y., Mahapatra, K., Trathan, P. N., Okazaki, M., Hayashi, T., & Okuda, T. (2020). Body length-dependent diel vertical migration of Antarctic krill in relation to food availability and predator avoidance in winter at South Georgia. *Marine Ecology Progress Series*, *654*, 53–66. https://doi.org/10.3354/meps13508

Jaffe, J. S., Ohman, M. D., & Robertis, A. D. (1999). Sonar estimates of daytime activity levels of *Euphausia pacifica* in Saanich Inlet. *Canadian Journal of Fisheries and Aquatic Sciences*, *56*(11), 2000–2010. https://doi.org/10.1139/f99-132

Kaartvedt, S. (2010). Diel vertical migration behaviour of the northern krill (*Meganyctiphanes norvegica* Sars). In G. A. Tarling (Ed.), *Advances in Marine Biology* (Vol. 57, pp. 255–275). Academic Press. https://doi.org/10.1016/B978-0-12-381308-4.00009-1

Kaartvedt, S., Larsen, T., Hjelmseth, K., & Onsrud, M. S. R. (2002). Is the omnivorous krill *Meganyctiphanes norvegica* primarily a selectively feeding carnivore? *Marine Ecology Progress Series*, *228*, 193–204. https://doi.org/10.3354/meps228193

Kaartvedt, S., Røstad, A., Fiksen, Ø., Melle, W., Torgersen, T., Breien, M. T., & Klevjer, T. A. (2005). Piscivorous fish patrol krill swarms. *Marine Ecology Progress Series*, *299*, 1–5. https://doi.org/10.3354/meps299001

Kaartvedt, S., Røstad, A., Klevjer, T. A., & Staby, A. (2009). Use of bottom-mounted echo sounders in exploring behavior of mesopelagic fishes. *Marine Ecology Progress Series*, *395*, 109–118. https://doi.org/10.3354/meps08174

Karlson, K., & Båmstedt, U. (1994). Planktivorous predation on copepods. Evaluation of mandible remains in predator guts as a quantitative estimate of predation. *Marine Ecology Progress Series*, *108*(1), 79–90.

Kattner, G., & Hagen, W. (2009). Lipids in marine copepods: Latitudinal characteristics and perspective to global warming. In M. Kainz, M. T. Brett, & M. T. Arts (Eds.), *Lipids in Aquatic Ecosystems* (pp. 257–280). Springer. https://doi.org/10.1007/978-0-387-89366-2_11

Kelley, D. E. (2018). The oce package. In D. E. Kelley (Ed.), *Oceanographic Analysis with R* (pp. 91–101). Springer. https://doi.org/10.1007/978-1-4939-8844-0_3

Kelley, D., & Richards, C. (2021). *oce: Analysis of oceanographic data* [Manual]. https://CRAN.R-project.org/package=oce

Klevjer, T. A., & Kaartvedt, S. (2003). Split-beam target tracking can be used to study the swimming behaviour of deep-living plankton in situ. *Aquatic Living Resources*, *16*(3), 293–298. Cambridge Core. https://doi.org/10.1016/S0990-7440(03)00013-5

Klevjer, T. A., & Kaartvedt, S. (2006). In situ target strength and behaviour of northern krill (*Meganyctiphanes norvegica*). *ICES Journal of Marine Science*, *63*(9), 1726–1735. https://doi.org/10.1016/j.icesjms.2006.06.013

Klevjer, T. A., & Kaartvedt, S. (2011). Krill (*Meganyctiphanes norvegica*) swim faster at night. *Limnology and Oceanography*, *56*. https://doi.org/10.4319/lo.2011.56.3.0765

Kongsberg Maritime. (n.d.). *Simrad WBAT Autonomous scientific echo sounder*. Kongsberg. Retrieved May 21, 2021, from https://www.kongsberg.com/no/maritime/products/mapping-systems/fishery-research/ekkolodd-for-fiskeri-forskning/wbat/

Koslow, J. A., Goericke, R., Lara-Lopez, A., & Watson, W. (2011). Impact of declining intermediate-water oxygen on deepwater fishes in the California Current. *Marine Ecology Progress Series*, *436*, 207–218. https://doi.org/10.3354/meps09270

Krebs, J. R., & Davies, N. B. (1978). *Behavioural ecology: An evolutionary approach*. Blackwell Scientific Publications.

Lee, R. F., & Hirota, J. (1973). Wax esters in tropical zooplankton and nekton and the geographical distribution of wax esters in marine copepods. *Limnology and Oceanography*, *18*(2), 227–239. https://doi.org/10.4319/lo.1973.18.2.0227

Levin, L. A. (2018). Manifestation, drivers, and emergence of open ocean deoxygenation. *Annual Review of Marine Science*, *10*(1), 229–260. https://doi.org/10.1146/annurev-marine-121916-063359

Nesje, A., & Whillans, I. M. (1994). Erosion of Sognefjord, Norway. *Geomorphology*, *9*(1), 33–45. https://doi.org/10.1016/0169-555X(94)90029-9

Netburn, A. N., & Koslow, J. A. (2015). Dissolved oxygen as a constraint on daytime deep scattering layer depth in the southern California current ecosystem. *Deep Sea Research Part I: Oceanographic Research Papers*, *104*, 149–158. https://doi.org/10.1016/j.dsr.2015.06.006

Nychka, D., Furrer, R., Paige, J., & Sain, S. (2017). *fields: Tools for spatial data*. https://doi.org/10.5065/D6W957CT

Ocean science systems. (n.d.). Retrieved October 3, 2021, from https://www.kongsberg.com/maritime/products/ocean-science/fishery-research/

Onsrud, M. S. R., & Kaartvedt, S. (1998). Diel vertical migration of the krill *Meganyctiphanes norvegica* in relation to physical environment, food and predators. *Marine Ecology Progress Series*, *171*, 209–219. https://doi.org/10.3354/meps171209

Pierce, D. (2019). *ncdf4: Interface to unidata netCDF (version 4 or earlier) format data files* [Manual]. https://CRAN.R-project.org/package=ncdf4

QGIS Development Team. (2021). *QGIS geographic information system* [Manual]. https://www.qgis.org

R Core Team. (2019). *R: A language and environment for statistical computing* [Manual]. https://www.R-project.org/

Ringelberg, J. (2010). *Diel Vertical Migration of Zooplankton in Lakes and Oceans: Causal explanations and adaptive significances* (1st ed. 2010.). Springer Netherlands: Imprint: Springer.

Riquelme-Bugueño, R., Pérez-Santos, I., Alegría, N., Vargas, C. A., Urbina, M. A., & Escribano, R. (2020). Diel vertical migration into anoxic and high-pCO2 waters: Acoustic and net-based krill observations in the Humboldt Current. *Scientific Reports*, *10*(1), 17181. https://doi.org/10.1038/s41598-020-73702-z

Rosenberg, R., Gray, J. S., Josefson, A. B., & Pearson, T. H. (1987). Petersen's benthic stations revisited. II. Is the Oslofjord and eastern Skagerrak enriched? *Journal of Experimental Marine Biology and Ecology*, *105*(2), 219–251. https://doi.org/10.1016/0022-0981(87)90174-2

Røstad, A., & Kaartvedt, S. (2013). Seasonal and diel patterns in sedimentary flux of krill fecal pellets recorded by an echo sounder. *Limnology and Oceanography*, *58*(6), 1985–1997. https://doi.org/10.4319/lo.2013.58.6.1985

RStudio Team. (2020). *RStudio: Integrated development environment for R* [Manual]. http://www.rstudio.com/

Saborowski, R., Salomon, M., & Buchholz, F. (2000). The physiological response of Northern krill (*Meganyctiphanes norvegica*) to temperature gradients in the Kattegat. *Hydrobiologia*, *426*(1), 157–160. https://doi.org/10.1023/A:1003974613473

SAIV A/S. (n.d.). *CTD profiler Model SD204—SAIV A/S*. Retrieved May 21, 2021, from https://saiv.no/sd204-ctd-profiler

Sato, M., Dower, J. F., Kunze, E., & Dewey, R. (2013). Second-order seasonal variability in diel vertical migration timing of euphausiids in a coastal inlet. *Marine Ecology Progress Series*, *480*, 39–56. https://doi.org/10.3354/meps10215

Schmidt, K. (2010). Food and feeding in northern krill (*Meganyctiphanes norvegica* Sars). In G. A. Tarling (Ed.), *Advances in Marine Biology* (Vol. 57, pp. 127–171). Academic Press. https://doi.org/10.1016/B978-0-12-381308-4.00005-4

Sea-Bird Scientific. (n.d.). *SBE 911plus CTD | Sea-Bird Scientific—Overview | Sea-Bird*. Retrieved May 21, 2021, from https://www.seabird.com/profiling/sbe-911plus-ctd/family?productCategoryId=54627473769

Sefick Jr., S. (2016). *Stream Metabolism-A package for calculating single station metabolism from diurnal Oxygen curves* [Manual]. https://cran.r-project.org/package=StreamMetabolism

Sievert, C. (2020). *Interactive web-based data visualization with r, plotly, and shiny*. Chapman and Hall/CRC. https://plotly-r.com

Simmonds, J., & MacLennan, D. (2006). *Fisheries Acoustics: Theory and Practice* (2nd edition). Wiley-Blackwell.

Simrad EK series. (n.d.). Retrieved October 3, 2021, from https://www.kongsberg.com/maritime/support/simradsupport/simrad-docs/discontinued-echo-sounders/simrad-ek500/

Solberg, I., Klevjer, T. A., & Kaartvedt, S. (2012). Continuous acoustic studies of overwintering sprat *Sprattus sprattus* reveal flexible behavior. *Marine Ecology Progress Series*, *464*, 245–256. https://doi.org/10.3354/meps09877

Solberg, I., Røstad, A., & Kaartvedt, S. (2015). Ecology of overwintering sprat (*Sprattus sprattus*). *Progress in Oceanography*, *138*, 116–135. https://doi.org/10.1016/j.pocean.2015.08.003

Sourisseau, M., Simard, Y., & Saucier, F. J. (2008). Krill diel vertical migration fine dynamics, nocturnal overturns, and their roles for aggregation in stratified flows. *Canadian Journal of Fisheries and Aquatic Sciences*, *65*(4), 574–587. https://doi.org/10.1139/f07-179

Spicer, J. I., & Saborowski, R. (2010). Physiology and metabolism of northern krill (*Meganyctiphanes norvegica* Sars). In G. A. Tarling (Ed.), *Advances in Marine Biology* (Vol. 57, pp. 91–126). Academic Press. https://doi.org/10.1016/B978-0-12-381308-4.00004-2

Spicer, J. I., Thomasson, M. A., & Strömberg, J.-O. (1999). Possessing a poor anaerobic capacity does not prevent the diel vertical migration of Nordic krill *Meganyctiphanes norvegica* into hypoxic waters. *Marine Ecology Progress Series*, *185*, 181–187. https://doi.org/10.3354/meps185181

Stramma, L., Schmidtko, S., Levin, L. A., & Johnson, G. C. (2010). Ocean oxygen minima expansions and their biological impacts. *Deep Sea Research Part I: Oceanographic Research Papers*, *57*(4), 587–595. https://doi.org/10.1016/j.dsr.2010.01.005

Strömberg, J.-O., & Spicer, J. I. (2000). Cold comfort for krill? Respiratory consequences of diel vertical migration by *Meganyctiphanes norvegica* into deep hypoxic waters. *Ophelia*, *53*(3), 213–217. https://doi.org/10.1080/00785326.2000.10409451

Stuart, V., & Pillar, S. C. (1990). Diel grazing patterns of all ontogenetic stages of *Euphausia lucens* and in situ predation rates on copepods in the southern Benguela upwelling region. *Marine Ecology Progress Series*, *64*(3), 227–241. JSTOR.

Sunrise and sunset times in Oslo, August 2020. (n.d.). Retrieved May 26, 2021, from https://www.timeanddate.com/sun/norway/oslo?month=8&year=2020

Sunrise and sunset times in Oslo, March 2020. (n.d.). Retrieved April 21, 2021, from https://www.timeanddate.com/sun/norway/oslo?month=3&year=2020

Sunrise and sunset times in Oslo, October 2020. (n.d.). Retrieved May 26, 2021, from https://www.timeanddate.com/sun/norway/oslo?month=10&year=2020

Tarling, G. A., Buchholz, F., & Matthews, J. B. L. (1999). The effect of a lunar eclipse on the vertical migration behaviour of *Meganyctiphanes norvegica* (Crustacea: Euphausiacea) in the Ligurian Sea. *Journal of Plankton Research*, *21*(8), 1475–1488. https://doi.org/10.1093/plankt/21.8.1475

Tarling, G. A., Ensor, N. S., Fregin, T., Goodall-Copestake, W. P., & Fretwell, P. (2010). An introduction to the biology of northern krill (*Meganyctiphanes norvegica* Sars). In G.

A. Tarling (Ed.), *Advances in Marine Biology* (Vol. 57, pp. 1–40). Academic Press. https://doi.org/10.1016/B978-0-12-381308-4.00001-7

Thomasson, M. A., Johnson, M. L., Strömberg, J.-O., & Gaten, E. (2003). Swimming capacity and pleopod beat rate as a function of sex, size and moult stage in Northern krill *Meganyctiphanes norvegica*. *Marine Ecology Progress Series*, *250*, 205–213. https://doi.org/10.3354/meps250205

Torgersen, T. (2001). Visual predation by the euphausiid *Meganyctiphanes norvegica*. *Marine Ecology Progress Series*, *209*, 295–299. https://doi.org/10.3354/meps209295

Torres, J. J., & Childress, J. J. (1983). Relationship of oxygen consumption to swimming speed in *Euphausia pacifica*. *Marine Biology*, *74*(1), 79–86. https://doi.org/10.1007/BF00394278

Tremblay, N., Hünerlage, K., & Werner, T. (2020). Hypoxia Tolerance of 10 Euphausiid Species in Relation to Vertical Temperature and Oxygen Gradients. *Frontiers in Physiology*, *11*, 248. https://doi.org/10.3389/fphys.2020.00248

Trevorrow, M. V. (2005). The use of moored inverted echo sounders for monitoring meso-zooplankton and fish near the ocean surface. *Canadian Journal of Fisheries and Aquatic Sciences*, *62*(5), 1004–1018. https://doi.org/10.1139/f05-013

Turner, J. T. (2002). Zooplankton fecal pellets, marine snow and sinking phytoplankton blooms. *Aquatic Microbial Ecology: International Journal*, *27*(1), 57–102. https://doi.org/10.3354/ame027057

US Department of Commerce, N. (n.d.). *ESRL Global Monitoring Laboratory—Global Radiation and Aerosols*. Retrieved October 5, 2021, from https://gml.noaa.gov/grad/solcalc/

Vestheim, H., Røstad, A., Klevjer, T. A., Solberg, I., & Kaartvedt, S. (2014). Vertical distribution and diel vertical migration of krill beneath snow-covered ice and in ice-

free waters. *Journal of Plankton Research*, *36*(2), 503–512. https://doi.org/10.1093/plankt/fbt112

Wickham, H. (2016). *ggplot2: Elegant graphics for data analysis*. Springer-Verlag New York. https://ggplot2.tidyverse.org

Wishner, K. F., Seibel, B. A., Roman, C., Deutsch, C., Outram, D., Shaw, C. T., Birk, M. A., Mislan, K. A. S., Adams, T. J., Moore, D., & Riley, S. (2018). Ocean deoxygenation and zooplankton: Very small oxygen differences matter. *Science Advances*, *4*(12), eaau5180. https://doi.org/10.1126/sciadv.aau5180

Appendix

Appendix A: Study area sunrise and sunset times in UTC

Table A 1. Retrieved sunrise/sunset times in the study area in times from March recording days, using Coordinated Universal Time (UTC).

March field campaign		
Date	Sunrise, in UTC	Sunset, in UTC
21.03.20	05:14:43	17:34:57
22.03.20	05:11:42	17:37:22
23.03.20	05:08:42	17:39:47
24.03.20	05:05:41	17:42:12
25.03.20	05:02:41	17:44:37
26.03.20	05:59:40	17:47:02

Table A 2. Retrieved sunrise/sunset times in UTC, in the study area, from August recording days.

August field campaign		
Date	Sunrise, local time	Sunset, local time
06.08.20	03:11:47	19:32:29
07.08.20	03:14:09	19:29:52
08.09.20	03:16:31	19:27:13
09.09.20	03:18:54	19:24:34
10.09.20	03:21:16	19:21:53

Table A 3. Retrieved sunrise/sunset times in UTC, in the study area, from October recording days.

October field campaign		
Date	Sunrise, local time	Sunset, local time
20.10.20	06:09:09	15:53:24
21.10.20	06:11:38	15:50:36
22.10.20	06:14:07	15:47:49

Appendix B: Manual sinking and swimming speeds from March

Table B 1. Krill traces physically measured from an echogram, sinking (March). R = range, t = time.

Trace	R_{start} (m)	t_{start} (UTC)	R_{end} (m)	t_{end} (UTC)	ΔR	Δt	Velocity ($m \cdot s^{-1}$)
1	14.10	12:02:39	13.11	12:06:07	0.99	00:03:28	$4.76 \cdot 10^{-3}$
2	26.95	12:02:03	25.10	12:07:33	1.85	00:05:30	$5.61 \cdot 10^{-3}$
3	28.59	12:03:53	25.05	12:12:10	3.45	00:08:17	$6.94 \cdot 10^{-3}$
4	40.63	12:03:19	38.94	12:06:41	1.69	00:03:22	$8.37 \cdot 10^{-3}$
5	34.26	12:09:06	32.49	12:12:17	1.77	00:03:11	$9.27 \cdot 10^{-3}$
6	26.64	08:02:56	25.24	08:05:55	1.40	00:02:59	$7.82 \cdot 10^{-3}$
7	24.13	08:34:15	19.44	08:43:01	4.69	00:08:46	$8.92 \cdot 10^{-3}$
8	18.61	09:17:58	16.60	09:23:05	2.01	00:05:07	$6.55 \cdot 10^{-3}$
9	31.46	09:39:41	28.23	09:48:00	3.23	00:08:19	$6.47 \cdot 10^{-3}$
10	20.89	09:58:21	18.72	10:03:34	2.17	00:05:13	$6.93 \cdot 10^{-3}$
11	33.16	14:47:31	29.18	15:57:37	3.98	00:10:06	$6.57 \cdot 10^{-3}$
12	31.54	15:13:05	28.43	15:23:05	3.11	00:10:00	$5.18 \cdot 10^{-3}$
13	35.02	15:27:50	32.49	15:33:45	2.53	00:05:55	$7.13 \cdot 10^{-3}$
14	38.14	16:05:28	34.14	16:13:17	3.19	00:07:49	$6.80 \cdot 10^{-3}$
15	32.27	16:08:28	29.62	16:16:50	2.65	00:08:22	$5.28 \cdot 10^{-3}$

Table B 2. Upwards moving traces with estimated velocties (March). R = range (m), t = time in UTC. N = 20.

Trace	R_{start} (m)	t_{start}	R_{end} (m)	t_{end}	ΔR (m)	Δt (sec)	Velocity ($m \cdot s^{-1}$)
1	8.03	07:39:30	10.01	07:40:50	1.98	80	0.02475
2	8.98	07:37:33	10.59	07:38:36	1.61	63	0.025556
3	13.08	08:04:15	15.20	08:06:19	2.12	124	0.0171
4	12.09	09:41:14	13.85	09:42:33	1.76	79	0.02266
5	10.63	10:25:50	13.99	10:28:06	3.36	136	0.02471
6	12.89	12:10:08	14.54	12:11:29	1.65	81	0.02037
7	13.46	12:58:06	14.18	12:58:43	0.72	37	0.01946
8	12.64	13:16:35	13.71	13:17:51	1.07	76	0.01408
9	20.96	14:04:48	21.97	14:05:47	1.01	59	0.01712
10	13.35	14:04:51	14.57	14:05:41	1.22	50	0.0244
11	10.84	14:08:16	12.28	14:09:57	1.44	101	0.01426
12	15.15	14:27:29	16.37	14:28:18	1.22	49	0.024898
13	21.18	14:28:50	22.19	14:29:36	1.01	46	0.02196
14	18.02	14:33:28	19.74	14:34:47	1.72	79	0.0218
15	15.38	12:38:31	16.64	12:39:34	1.31	63	0.02079
16	18.10	07:15:32	19.79	07:16:43	1.69	71	0.0238
17	12.96	10:52:09	13.87	10:52:53	0.91	44	0.02068
18	16.73	11:01:33	17.90	11:02:40	1.17	67	0.01746
19	12.11	11:22:27	13.09	11:23:15	0.98	48	0.0204
20	21.41	11:19:55	22.84	11:20:59	1.43	64	0.0223

Appendix C: Krill sizes

Table C 1. Krill total lengths from August krill sampling.

	Depth (m)					
	70	80	90	100	120	140
Individual	Total length (mm)					
1	32	28	32	28	34	34
2	36	33	33	35	35	33
3	32	36	17	35	34	33
4	33	33	36	30	34	32
5	34	30	34	31	27	33
6	35	39	32	27	34	32
7	33	35	33	31	33	34
8	32	33	35	33	35	33
9	35	37	29	36	31	34
10	34	34	38	35	28	30
11	37	33	30	29	34	34
12	36	36	29	26	33	32
13	30	37	33	31	32	29
14	34	31	33	30	28	33
15	35	33	30	33	33	35
16	30	35	36	32	32	32
17	34	33	35	33	28	32
18	40	33	28	30	31	31
19	33	38	36	33	33	35
20	32	34	35	32	30	28
21	28	27	28	36	32	28
22	33	29	27	26	30	31
23	34	29	33	28	30	27
24	27	34	30	34	32	32
25	35	34	30	29	28	30
26	35	32	33	26	32	33
27	32	33	33	30	32	30
28	34	29	34	30	31	32
29	33	35	33	28	33	32
30	33	32	34	31	29	28
31	32	33	34	34	30	29
32	33	28	33	38	31	28
33	32	37	33	30	30	31
34	34	34	33	30	30	31
35	33	34	30	32	31	29
36	37	34	28	35	34	32
37	32	36	28	32	30	38
38	34	31	32	32	32	38
39	34	32	35	28	28	31
40	34	32	35	33	32	33
41	38	32	28	34	32	33
42	34	35	29	33	31	32
43	34	30	33	27	25	26
44	34	34	33	32	27	33
45	32	36	31	28	30	38
46	34	32	33	30	30	30
47	34	32	33	28	31	33
48	29	32	33	32	35	29
49	33	36	35	34	33	28
50	34	35	34	27	33	29

Table C 2. Lengths measured from October krill sampling. 7 last counted individuals in sample from 130 m not included because sizes are NA due do breakage of bodies during sampling.

			Depth (m)	
	70	90	115	130
Individuals			Total length (mm)	
1	31	29	35	32
2	30	27	32	33
3	29	33	35	34
4	32	28	32	26
5	32	32	33	30
6	35	29	33	31
7	33	15	33	30
8	33	31	33	31
9	32	32	30	34
10	31	32	30	35
11	30	32	32	33
12	30	30	33	32
13	31	28	31	33
14	31	29	34	34
15	31	31	33	32
16	33	29	37	33
17	33	32	34	31
18	34	33	30	32
19	32	30	30	32
20	33	33	32	30
21	32	28	31	35
22	30	32	NA	28
23	34	33	34	35
24	30	30	31	33
25	31	30	32	34
26	28	30	31	36
27	32	30	33	32
28	31	30	36	35
29	34	30	35	29
30	28	34	30	30
31	34	30	20	33
32	29	31	32	32
33	36	31	30	30
34	30	31	33	32
35	33	29	35	30
36	32	33	35	30
37	34	28	35	32
38	35	30	34	32
39	31	26	35	31
40	35	33	33	31
41	32	31	33	34
42	27	31	32	33
43	30	30	30	33
44	34	27	35	34
45	41	35	32	30
46	32	31	34	29
47	31	32	31	32
48	30	31	34	33
49	34	29	32	31
50	29	33	36	37
51				30

52	34
53	34
54	32
55	33
56	34
57	34
58	34
59	35
60	31
61	32
62	18
63	32
64	29
65	28
66	31

Appendix D: R scripts

Code in **bold**, information marked with #, and headers marked with ##

```
## Scripts (with explanations) that was used for acoustic backscattering
data was taught and originally written by by Doctoral research fellow
Svenja Christiansen, and further developed and explained by Fredrik Lund
Moksnes (author of this thesis) and modified to fit data analysis.

## How to make an echogram showing one (or a specified part of a) day's
recording with the WBAT using gridded data. Example from March recordings:

# First, we start off by loading necessary packages:

library(ncdf4)

# This package reads and writes .nc files, which is necessary to work with
the gridded data.

library(fields)

# This package has useful plot functions for spatial data that we can
utilize when for example making echograms, with color variations and
supplemented with color strips.

library(lattice)

# Also, a package useful for graphics.

fileName = "C:\\example_nc_file.nc"

# Here we type in the the path to the location where we have stored the .nc
datafile on our computer.

nc_data = nc_open(fileName)

# Opens the datafile

Range = ncvar_get(nc_data, "Range")

# Range from the echosounder in meters

Daytime = ncvar_get(nc_data, "Daytime")

# Daytime as decimal between 0 and 1, where 0 and 1 are midnight and 0.5 is
noon.

Date = ncvar_get(nc_data,"Date")

# The date in a matlab format, which we will convert to another format
further down in the script.

Sv = ncvar_get(nc_data, "Sv")

# Backscatter (Sv) in decibels (dB). This is a three-dimensional matrix
with one dimension for the range, one for the daytime and one for the date.

nc_close(nc_data)
```

```
# Closes the datafile

Depth = rev(Range)

#Here we turn the range in to depth by reversing it.

Dates_converted = as.POSIXct(((Date - 719529) * 86400), origin = '1970-1-
1',tz = 'UTC')

# Converts dates from the matlab format into POSIXct, which is date format
more commonly used in R.

whichday = as.POSIXct("2020-03-22",tz = "UTC")

# Selects a particular date from our data and convert it to a POSIXct
format

Sv_use = Sv[,,Dates_converted == whichday]

# This tells R that we only want backscatter data from the date that we
selected

Sv_use = drop(Sv_use)

# Gets rid of extra dimensions so that we get a two-dimensional matrix that
we can plot into an echogram.
```

```
# Now we are ready to plot the backscatter (Sv) data into an image with
depth over time, making an echogram by using the image.plot function.

image.plot(Daytime, -Depth,t(Sv_use[-1,-1]),zlim = c(-85,-50),xlim =
c(0,1),ylim = c(-150,0),oldstyle = T,

           smallplot = c(.89, .94, .2, .8),

           axes = F,

           ylab = "",

           xlab = "")

axis(side=2, at = seq(-150, 0, by=30), las=2, labels = c("150",
"120","90","60", "30", "0"))

mtext("Depth (m)", side = 2, line=3, font=2)

axis(side = 1, at = c(0.0,0.25,0.5,0.75,1), las=1, labels =
(c("00:00","06:00","12:00","18:00","24:00")))

mtext("Time of Day (UTC)", side = 1, line=4, font=2)

axis(side = 3, at = c(0.2166667, 0.7340278), las=1, labels = c("☼", "☽"))

mtext("Sv (dB)", side = 3, las=1, font = 1, line = 1, at = 1.12)

# The t() argument is here important, to prevent that the echogram is not
displayed upside down.

# ylim and xlim can modify limits of the plot axes. By adjusting these we
can zoom into parts of the echogram.

# The “Depth” variable must be entered with a negative pre-sign

# The smallplot() function defines the colorstip dimensions.

# We leave axes and axis labels empty so that we can manually define these
outside of the plot command by adding axis() and mtext()
```

```
## How to make an echogram plot covering multiple days of recording:

whichdays = Dates_converted

Sv_use_more = c()

# An empty array, that will be filled in loop

datetimevec = as.POSIXct(rep(Daytime[-1],length(whichdays)) *(24*60*60) +
as.numeric(rep(whichdays,each = length(Daytime[-1]))),origin = '1970-1-
1',tz = 'UTC')

# Combine a time vector with dates, exclude last time since (0 = 1 =
midnight)

for (d in whichdays){

  tmp = Sv[,,Dates_converted == d]

  Sv_use_more = cbind(Sv_use_more[,-1],drop(tmp))

}

# A foreloop to tell R that we only want the backscatter data from the date
that was just defined

# Append current data to matrix, exclude last column (0 = 1 = midnight),
use drop() to get rid of extra dimensions to get a 2D matrix which we can
plot and work with.

image.plot(datetimevec, -Depth1,

           t(Sv_use_more[-1,-1]), zlim = c(-85,-50),

           axes = F,

           ylab = "",

           xlab = "")

axis(side=2, at = seq(-150, 0, by=30), las=2, labels =
as.character(abs(seq(-150, 0, by=30))))

mtext("Depth (m)", side = 2, las = 0, line=3, font=2)

axis(side = 1, at = whichdays, las = 1, labels = c("Sat (21.03)","Sun
(22.03)","Mon (23.03)","Tue (24.03)","Wed (25.03)","Thu (26.03)"))

mtext("Sv (dB)", side = 3, las=1, font = 1, line = 1, adj = 1)



## How to make a plot using sample data from Sonar5-Pro:

# By using the export function in Sonar5-Pro, we can export data as a .txt
file from a part of an echogram that we have zoomed in on. Example from
October data zoomed in on a ~120 m depth limit where krill did not travel
below, due to the constricting oxygen in the area:
```

```
Filename = "D:\\R_data\\Zoom-ins\\M_Oslofjord_200kHz_20201020-Phase0-
D20201021-T000740-90-pp_R_0-160_P63079-64030_R29.82-37.92.txt"

data = read.csv(filename, header = T, sep = "\t", skip = 40, fileEncoding =
"UTF-8", skipNul = T)

# The first rows of the file are headers and information and should be
skipped down to where the observations are.

data[data == -900] = NA

# Replaces values of -900 in the data file by NA, which is many.

echogram = as.matrix(data[,5:ncol(data)])

# This transforms the data frame into a matrix

minrange = 29

maxrange = 38

# The header of the file provides the lowest and the largest range in the
sample, so that we can define this in the script.

ranges = linspace(minrange,maxrange,ncol(data)-4)

# This makes an evenly spaced vector containing the ranges from minimum to
maximum.

times = as.POSIXct(data$Time..hh.mm.ss.hhh.,"%H:%M:%OS",tz="UTC")

# set HMS time format from the time variable in the datafile.

#The plot command then becomes:

image.plot(times,ranges,echogram,zlim = c(-85,-50),xlim =
c(times[1],times[951]),ylim =c(29,38),oldstyle = T,

           smallplot = c(.89, .94, .2, .8),

           xlab = "",

           ylab = "",

           axes = F)

axis(side = 2, at = seq(29, 38, by= 1), labels = 150-seq(29, 38, by= 1),
las=1)

mtext("Depth (m)", side = 2, line = 3, font = 2)

axis(side = 1, at = seq(round.POSIXt(times[1], units =
"mins"),round.POSIXt(times[951], units = "mins"), by = 120),

     labels = c("11:29","11:31","11:33","11:35","11:37","11:39"))

mtext("Time (UTC)", side = 1, line = 4, font = 2)

mtext("Sv (dB)", side = 3, las=1, font = 1, line = 1, adj = 1)
```

```
## How to make a 3D plot using with plotly using sample data from target
tracking in Sonar-5 Pro. Example used from sinking track in March data:

library(plotly)

library(zoo)

df = "D:\\R_data\\Individuals\\Automatic Target
Tracking\\ET20210921152208_Tracks_Echo_information.txt"

tracks = read.csv(df, sep = "\t", dec = ".", skip = 35, header = T)

#Add depth of the echosounder:

Echosounder_depth = 154

# Select the track we want from the fish basket textfile generated in
Sonar5-Pro:

tracks_subset = tracks[tracks$Track.Index ==1,]

tracks_subset$Depth = Echosounder_depth - tracks_subset$R.m.

#Make a foreloop with na.approx() to interpolate all NAs:

for (i in 1:ncol(tracks_subset)) {tracks_subset[,i] = na.approx(object =
tracks_subset[,i], na.rm = F)

}

#In order to display a path for the 3D track I had to manually select rows
without NAs still appearing in the data.frame

tracks_subset_subset = tracks_subset[c(26:166),]

#Manually setting axis labels for plot_ly():

axx = list(

  title = "X (m)"

)

axy = list(

  title = "Y (m)"

)



axz = list(

  title = "Depth (m)"

)
```

```
# Plot_ly() command displays 3D-model that is easily rotatable through
point-and-click

plot_ly(tracks_subset_subset, x = ~X.m., y = ~Y.m., z = ~Depth, type =
'scatter3d', mode = 'lines+markers',

               line = list(width = 6, color = ~c, colorscale = 'Viridis'),

               marker = list(size = 3.5, color = ~c, colorscale = 'Greens',
cmin = -20, cmax = 50)) %>%

  layout(

    scene = list(xaxis=axx,yaxis=axy,zaxis=axz))

## How to retrieve sunrise and sunset in Bunnefjord, in UTC:

library(StreamMetabolism)

# This package has a function that can retrieve data from a sunrise and
sunset calculator (NOAA)

sunrise.set(59.79333, +10.7180, "2020/03/21", timezone = "UTC", num.days =
6)

# In the example, I used recording days from our March campaign. All that
is required is the coordinates in decimal degrees (DD), date, timezone, and
a number of days forward from the date. This generates a table of sunrise
and sunset times.



## How to present our catch data, size measurements, and stomach analysis:

library(tidyverse)

library(RColorBrewer)

library(patchwork)

library(hrbrthemes)

library(ggeasy)

# Using our August catches as an example, a tab derived .txt file converted
from excel:

# Set the file path:

datafile = "D:\\lab work\\krill
measurings\\Krill_lengdemålinger_11aug2020_mod1.txt"

# read the data:

augmeas = read.csv(datafile, header = T, sep = "\t", dec = ",",
stringsAsFactors = F)[-c(1),]

#Convert variables into numeric values:
```

```
augmeas$Individual = as.numeric(as.character(augmeas$Individual))

augmeas$Depth_Z_.m. = as.numeric(as.integer(augmeas$Depth_Z_.m.))

augmeas$Total_length_TL_.mm. =
as.numeric(as.character(augmeas$Total_length_TL_.mm.))

augmeas$Total_catch = as.numeric(as.character(augmeas$Total_catch))



subset_catch = augmeas[c(2, 52, 102, 152,201,202,252,253),]

# Because ggplot (R) treated all Total_catch entries in each rows as one
observation and adds all these together, it was necessary to generate a
subset by selecting a row from each sample to visualize the correct catch
sizes. Some of the rows were empty observations to make plotting with a
more precise visualization of depth easier.

## Catch size plot:

ggplot(data = subset_catch, mapping = aes(x = Total_catch, y =
factor(Depth_Z_.m.), fill = Depth_Z_.m.)) +

  geom_col() +

  ggtitle("Catch sizes") +

  xlab("Number of individuals")+

  ylab("Depth (m)")+

  labs(fill = "Depth (m)")+

  scale_fill_gradient(low = "lightblue", high = "darkblue", guide = TRUE)+

  theme_bw() +

  theme(legend.position = "none") +

  scale_y_discrete(limits = rev)+

  guides(fill = guide_legend(reverse = F)) +

  ggeasy::easy_center_title()



## Size distributions:

ggplot(data = augmeas, aes(x = Total_length_TL_.mm., y =
factor(Depth_Z_.m.), fill = Depth_Z_.m.)) +

  geom_boxplot() +

  ggtitle("Size distribution, by sampling depths")+

  xlab("Total length (mm)") +
```

```
  ylab("Depth (m)") +

  theme_bw()+

  theme(legend.position ="none") +

  labs(fill = "Depth (m)") +

  scale_y_discrete(limits = rev) +

  guides(fill = guide_legend(reverse = F)) +

  scale_fill_gradient(low="lightblue",high="darkblue")+

  xlim(15, 45)+

  ggeasy::easy_center_title()

#Boxplot using sample depth as a factor variable. This was necessary to
tell ggplot (R) that the y-axis values are not numeric values to be taken
into the calculation.

#ANOVA test:

anova_test = anova(lm(Total_length_TL_.mm. ~ factor(Depth_Z_.m.), data =
augmeas))

#Pairwise t-test:

pairwise.t.test(augmeas$Total_length_TL_.mm., augmeas$Depth_Z_.m., p.adj =
"none")

#Averages and standard deviations:

Mean()

Sd()

## Stomach analysis; mandible observations:

df= "D:\\lab work\\krill measurings\\Mandibler_11aug2020_1.txt"

mandibles = read.csv(df, header = T, sep = "\t", stringsAsFactors = F)

mandibles$Observed_number_mandibles =
as.numeric(as.integer(mandibles$Observed_number_mandibles))



#Plotting the mandible observations into a barplot:

ggplot(data = mandibles, aes(x = Observed_number_mandibles, y =
factor(Depth_Z_.m.), fill = Depth_Z_.m.)) +

  geom_bar(stat = 'identity') +

  ggtitle("Mandibles by sample depth")+

  xlab("Observed mandibles") +
```

```
  ylab("Depth (m)") +

  theme_bw()+

  theme(legend.position = "none") +

  labs(fill = "Depth (m)") +

  scale_y_discrete(limits = rev) +

  guides(fill = guide_legend(reverse = F)) +

  scale_fill_gradient(low="lightblue",high="darkblue")+

  ggeasy::easy_center_title()


## Presenting our CTD profiles:

# For CTD collected using SBE:

library(oce)

library(sf)

# The oce package can work directly with .cnv files, which was collected
from SBE software. It also have useful functions for smoothening noisy
data, example from March:

ctd.file = "D:\\R_data\\CTD data vår og
sommer\\CTD\\CTD\\09032020\\Bunnefjord\\Bunnefjord 09032020_down.cnv"

ctd1 =read.ctd(ctd.file)

ctd_smooth1 = ctdDecimate(ctd1)

# For CTD using SD204, example from October, here we had .txt files to work
with and use generic R functions to filter the data. This was necessary
because the probe had not been emptied of old data, and subsequently
getting a profile of the downcast or upcast. We used the upcast:

datafile = "D:\\R_data\\CTD\\Bunnefjord_20201020_STD.txt"

oct_ctd = read.csv(datafile, skip = 11, header = T, sep = ";", dec = ",",
stringsAsFactors = F)

oct_trimmed2 = oct_ctd[-c(1:2149),]

## The following plot command script is modified from an R script provided
by MSc Therese Andersen, and originally written by an unknown researcher at
NIVA:

# Following the example of October CTD collection with SD204:

attach(oct_trimmed2)

par(oma=c(5,3,8,5), bg="white")
```

```
par(mex=0.8)

plot(Temp,Press, type="l", lty=1, lwd=2, col="red", ylim=rev(range(1:150)),
ylab=' ',xlab = "Temperature (°C)", col.lab = "red", font.lab = 2,
yaxt='n', yaxs="i", xlim = c(0,25))

axis(side=2, at=seq(0,150, by=30), las=2)

mtext("Depth (m)", 2, line=4, font=2)

par(new=TRUE)

plot.default(Sal., Press, ylim=rev(range(1:150)), col="royalblue1",
ann=FALSE, yaxt="n", xaxt="n", type="l", lty=1, yaxs="i", lwd=2, xlim =
c(20,34))

axis(3)

mtext("Practical salinity (PSU)", 3, line=3, font=2, col = "royalblue1")

par(new=TRUE)

plot.default(mg.l, Press, ylim=rev(range(1:150)), col="orange1", ann=FALSE,
yaxt="n", xaxt="n", type="l", lty=1, yaxs="i", lwd=2, xlim = c(0,10))

axis(side=3, pos = -30)

mtext("Dissolved oxygen (mg/l)", 3, line=7, font=2, col = "orange1")
```